Output Regulation and Tracking for Linear ODE-Hyperbolic PDE-ODE systems

Jeanne Redaud, Jean Auriol, Federico Bribiesca Argomedo

Output Regulation and Tracking for Linear ODE-Hyperbolic PDE-ODE systems

Jeanne Redaud [a] , Federico Bribiesca-Argomedo [b], Jean Auriol [a]

[a] *Université Paris-Saclay, CNRS, CentraleSupélec, Laboratoire des Signaux et Systèmes, 91190, Gif-sur-Yvette, France*

[b] *Univ Lyon, INSA Lyon, Université Claude Bernard Lyon 1, Ecole Centrale de Lyon, CNRS, Ampère, UMR5005, 69621 Villeurbanne, France*

Abstract

This paper proposes a constructive solution to the output regulation - output tracking problem for a general class of interconnected systems. The class of systems under consideration consists of a linear 2×2 hyperbolic Partial Differential Equations (PDE) system coupled at both ends with Ordinary Differential Equations (ODEs). The proximal ODE system, which represents actuator dynamics, is actuated. Colocated measurements are available. The distal ODE system represents the load dynamics. The control objective is to ensure, in the presence of a disturbance signal (regulation problem), that a virtual output exponentially converges to zero. By doing so, we can ensure that a state component of the distal ODE state robustly converges towards a known reference trajectory (output tracking problem) even in the presence of a disturbance with a known structure. The proposed approach combines the backstepping methodology and frequency analysis techniques. We first map the original system to a simpler target system using an invertible integral change of coordinates. From there, we design an adequate full-state feedback controller in the frequency domain. Following a similar approach, we propose a state observer that estimates the state and reconstructs the disturbance from the available measurement. Combining the full-state feedback controller with the state estimation results in a dynamic output-feedback control law. Finally, existing filtering techniques guarantee the closed-loop system robustness properties.

Key words: Hyperbolic Partial Differential Equations, Infinite Dimensional systems, Distributed Parameter Systems, robust tracking, output regulation

1 Introduction

This paper considers a linear first-order hyperbolic PDE system interconnected at both ends of its spatial domain with an ODE. At the actuated end, the proximal ODE system represents actuator dynamics; on the opposite end, the distal ODE system represents the load dynamics. Both ODEs and PDE systems are potentially unstable. We propose an *observer-based, dynamic output-feedback controller* acting only on the proximal ODE system, which will guarantee that a prescribed output follows a reference trajectory. This output depends on the distal ODE states, which can be subject to exogenous disturbances.

Transport phenomena and delays are common in industrial applications. Therefore, many systems can be modeled by hyperbolic PDEs, for instance, oil drilling pipes [2,41], pneumatic systems [29], networks of hydraulic distribution lines or electrical lines [11,35]. Such systems can be coupled with finite-dimensional systems representing load or actuator dynamics. In the mentioned applications, the distal ODE state (i.e., the unactuated ODE) can model the Bottom Hole Assembly (BHA) at the end of a drilling pipe [9], currents in an inductor/voltage across a capacitor, or the dynamics of a suspended object for Unmanned Aerial Vehicles (UAV) [24]. More specifically, the ODE-PDE-ODE structure naturally arises when considering linear systems of balance laws with finite-dimensional actuator and load dynamics, as for the UAV-cable-payload structure [41], mining cable elevators [42] or the top drive electrical motor-drill pipes-BHA structure [34].

Due to the broad applicability of such interconnected systems, their analysis has been an active research field during the last few years. Independently controlling each subsystem of the chain is an easy task. Classical solutions such as

⋆ An earlier version of part of this work was presented at the 3rd DECOD Workshop.

Email addresses: jeanne.redaud@centralesupelec.fr (Jeanne Redaud), federico.bribiesca-argomedo@insa-lyon.fr (Federico Bribiesca-Argomedo), jean.auriol@centralesupelec.fr (Jean Auriol).

Smith Predictor controllers [36] can stabilize linear ODEs with input delays. Coupled hyperbolic PDE systems can also be stabilized by controllers based on the backstepping methodology [30,14]. Finally, the output regulation for a simple 2×2 linear hyperbolic system has been solved in [1]. When ODEs and PDEs are interconnected, and only one subsystem is actuated, solving the output tracking problem is much harder. The backstepping method has progressively been adapted to networks, with linear [20] and semilinear [37,27] hyperbolic PDE-ODE interconnections. Next, some results have been obtained for ODE-PDE-ODE interconnections [44,43], where full-state feedback controllers have been designed for such coupled systems [23,18]. In most cases, the constructive design is based on several invertible backstepping transforms [12,19]. In addition, output regulation and output tracking problems have been solved for interconnected systems. It is necessary for applications such as drilling [34] since the objective here is to impose a specific trajectory to the unactuated device at the end of the chain in the presence of disturbances. Some results have been obtained for cascaded networks of hyperbolic systems using PI controllers [38]. The backstepping approach has been recently used to solve disturbance rejection and output tracking problems for general linear heterodirectional hyperbolic systems [15,16], coupled linear wave–ODE systems [17], or hyperbolic PDE - nonlinear ODE systems [28]. Finally, it is important to mention that some backstepping-based approaches have led to non-proper controllers, which may be non-robust to delays [32]. Thus, it is crucial to ensure that the proposed controllers are robust to small delays, noise, or unavoidable small uncertainties. The robustness of stabilizing controllers for ODE-PDE-ODE systems has been addressed in [21,13]. Recently, a simple filtering method has been proposed in [6] to robustify non-proper stabilizing controllers by making them strictly proper using low-pass filters. This technique will be used in this paper to guarantee the robustness of the proposed control law and observer.

More specifically, our main contribution lies in a constructive approach to design a robust, dynamic output-feedback controller solving output regulation and output tracking for a wide class of interconnected ODE-hyperbolic PDE-ODE systems. Based on some structural assumptions and inspired by [13], we first design a full-state feedback controller stabilizing an output depending on the states of the distal ODE. The initial system is dynamically augmented with finite-dimensional exo-systems representing the reference trajectory and disturbance dynamics. We follow the backstepping methodology and use a general invertible integral transform to map this augmented system to a target system. Under structural assumptions similar to those found in [41], we then design a state observer for the augmented system, reconstructing the system states and the disturbance. The proposed approach only relies on a single-state transformation, which facilitates the implementation. Moreover, the controller and observer designs are based on assumptions that can be directly verified. We use filtering techniques [6] to guarantee the robustness of the proposed control law. Finally, the full-state feedback controller and the observer are coupled to obtain the dynamic output-feedback controller. Compared to existing results from the literature [13,6,41,15], our approach features several novelties. First, compared to [41], we do not want to stabilize the equilibrium or origin of the system but to make a virtual output converge to zero in the presence of disturbances or reference trajectories. As a result, in general, the system states still vary with time. Then, the observer design (that consists in stabilizing an error system) is not directly dual to the controller design. The existence of the disturbance, which the observer must estimate, makes the application of the filtering technique presented in [6] not straightforward since arbitrary low-pass filtering would result in a frequency-dependent phase shift in the reconstructed signals which would not allow for the exponential disturbance rejection. If the filtering technique from [6] was directly applied, we could just guarantee a practical convergence, and a small error would remain in the reconstruction of the exosystem. Our approach takes advantage of the knowledge of the disturbance and reference trajectory dynamical model to guarantee that no residual term remains that could impact the output feedback control law. Compared to [41], where the authors used measures of (potentially high-order) derivatives of the measured output, we only use a stable and strictly proper filter of this measurement. These robustness aspects are also a novelty compared to [15].

The layout of this paper is the following: first, we present in Section 2 the class of systems under consideration and give some structural assumptions. Next, we design in Section 3 a robust full-state feedback controller for output regulation. In Section 4, we propose an observer design for state estimation and disturbance reconstruction. This observer is used to obtain a dynamic output-feedback controller. Finally, we illustrate the performance of the proposed approach with some simulation results in Section 5.

Notation

In the following, we denote $\mathcal{T}^+$ the upper-triangular domain defined in $\mathbb{R}^2$ by $\mathcal{T}^+ \doteq \{(x,y) \in [0,1]^2, y \geq x\}$. Analogously, the lower-triangular domain of the unit square is denoted $\mathcal{T}^-$. Given a set $[a,b] \subset \mathbb{R}$, the characteristic function is defined by $\mathbb{1}_{[a,b]}(x) \doteq 1$ if $x \in [a,b]$ and 0 otherwise. The L_2-norm $\|\phi\|_{L^2}$ of a function $\phi \in L^2([0,1];\mathbb{R}^2)$ and the euclidean norm $\|\varphi\|_{\mathbb{R}^r}$ of a vector $\varphi \in \mathbb{R}^r$ are taken in the usual sense. We denote $\mathcal{X} \doteq \mathbb{R}^n \times L^2([0,1];\mathbb{R}^2) \times \mathbb{R}^{m+p}$ the space of the system states $(X(t), u(t,\cdot), v(t,\cdot), Y(t))$ (that will be defined later), and define the associated $\mathcal{X}-$norm as $\|(X,u,v,Y)\|_{\mathcal{X}} \doteq (\|X\|^2_{\mathbb{R}^n} + \|Y\|^2_{\mathbb{R}^{m+p}} + \|(u,v)\|^2_{L^2})^{\frac{1}{2}}$. We denote s the Laplace variable. For the sake of readability, we denote $\phi(s)$ the Laplace transform of $\phi(t)$. For any proper and stable transfer matrix $G(s)$, $\bar{\sigma}(G(j\omega))$ stands for the largest singular value of $G(j\omega)$ at frequency ω, and the H_∞-norm of G is $\|G\|_\infty = \operatorname{ess\,sup}_{\omega \in \mathbb{R}} \bar{\sigma}(G(j\omega))$. For any $q \in \mathbb{N}\backslash\{0\}$, we denote I_q the $q \times q$ identity matrix. If the dimensions are not ambiguous, the subindex may be omitted. The transpose of any matrix A is denoted A^T.

2 Problem Statement

In this section, we present the system under consideration. Then, we outline the control strategy and give some structural assumptions required to implement the proposed approach. We also discuss the conservatism of the assumptions.

2.1 System presentation

Consider a linear 2×2 hetero-directional hyperbolic PDE system coupled at both ends with ODEs. The proximal ODE system, which represents the actuator's dynamics, is actuated by a control input $U(t) \in \mathbb{R}^{c\times 1}$. Its state is denoted $X(t) \in \mathbb{R}^{n\times 1}$. The distal ODE system corresponds to the dynamics of the load, whose state is denoted $Y_1(t) \in \mathbb{R}^{m\times 1}$. This ODE is dynamically augmented by an exo-system, whose state is denoted $Y_2(t) \in \mathbb{R}^{p\times 1}$, such that $Y(t) = \left(Y_1(t) \mid Y_2(t)\right)^T \in \mathbb{R}^{(m+p)\times 1}$. The exogenous input can be considered either as a disturbance Y_{pert} and/or as a known reference trajectory Y_{ref}, depending on the control objective, as seen in Section 5. The PDE states are denoted $(u(t,x), v(t,x))$, $(t,x) \in [0,+\infty) \times [0,1]$. The resulting interconnected system is schematically represented in Figure 1. The states satisfy the equations

$$\dot{X}(t) = A_0 X(t) + E_0 v(t,0) + B_0 U(t), \tag{1}$$
$$u_t(t,x) + \lambda u_x(t,x) = \sigma^+(x) v(t,x), \tag{2}$$
$$v_t(t,x) - \mu v_x(t,x) = \sigma^-(x) u(t,x), \tag{3}$$
$$\dot{Y}(t) = A_1 Y(t) + \begin{pmatrix} E_1 \\ 0_{p\times 1} \end{pmatrix} u(t,1), \; A_1 = \begin{pmatrix} A_{11} & A_{12} \\ 0_{p\times m} & A_{22} \end{pmatrix} \tag{4}$$

with boundary conditions

$$v(t,1) = \rho u(t,1) + C_1 Y(t), \tag{5}$$
$$u(t,0) = q v(t,0) + C_0 X(t), \tag{6}$$

where $A_0 \in \mathbb{R}^{n\times n}$, $E_0 \in \mathbb{R}^{n\times 1}$, $B_0 \in \mathbb{R}^{n\times c}$, $A_{11} \in \mathbb{R}^{m\times m}$, $A_{12} \in \mathbb{R}^{m\times p}$, $A_{22} \in \mathbb{R}^{p\times p}$, $E_1 \in \mathbb{R}^{m\times 1}$, $C_0 \in \mathbb{R}^{1\times n}$, $C_1 = [C_{11}\ C_{12}]$, with $C_{11} \in \mathbb{R}^{1\times m}$ and $C_{12} \in \mathbb{R}^{1\times p}$. For the sake of simplicity, we suppose that the transport velocities $\lambda, \mu > 0$ are constant. The extension to space-dependent transport velocities is relatively straightforward yet complicates the computations and expressions [39]. While the boundary couplings $q, \rho \in \mathbb{R}$ are assumed constant, the in-domain couplings between the PDEs $\sigma^+, \sigma^- \in C([0,1];\mathbb{R})$ are space-dependent functions. Note that the diagonal coupling terms in the PDEs are not considered herein since they can be straightforwardly transferred to the anti-diagonal terms using a change of variables [10]. The initial condition associated to system (1)-(6) is denoted (X_0, u_0, v_0, Y_0) and belongs to $\mathcal{X}$. The open-loop system (1)-(6) is well-posed in the sense of the weak formulation [11, Appendix A]. We assume that we have access to a measurement of the proximal ODE state, such that $y(t) = C_{\text{mes}} X(t) \in \mathbb{R}^{n'\times 1}$. This structure is chosen since, in many applications [41,42,34], a measurement is available at the actuated end. However, the observer design would follow the same procedure if the measurements were available at the opposite end, only flipping the spatial variable and adapting the matrices used in the assumptions.

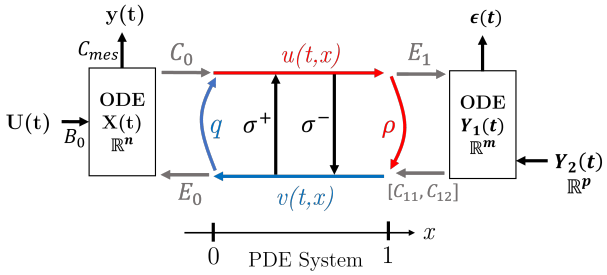

Fig. 1. Schematic presentation of the system

2.2 Control strategy

Our main objective is to design a controller $U(t)$ stabilizing a virtual output $\epsilon(t)$ defined by $\epsilon(t) \doteq C_e Y(t)$, with $C_e = [C_{e1}\ C_{e2}]$. In most cases, $\epsilon(t) \in \mathbb{R}$ is a scalar function, such that $C_{e1} \in \mathbb{R}^{1\times m}$, $C_{e2} \in \mathbb{R}^{1\times p}$ and we can only stabilize a linear combination of components of the extended state. The regulation to zero of this virtual input ϵ fulfills the trajectory tracking and disturbance rejection objectives. Two very simple examples of possible output definitions include:

- Taking $C_{e1} \neq 0_{\mathbb{R}^m}$, $C_{e2} = 0_{\mathbb{R}^p}$, we regulate to zero a linear combination of components of $Y_1(t)$ in the presence of a disturbance $Y_2(t)$, and solve an output regulation problem;
- Taking $C_{e1,i} - C_{e2,j} = 0$, $(i,j) \in [\![1,m]\!] \times [\![1,p]\!]$ (and the other components of the extended state equal to zero), we make the ith component of the output Y_1 converge towards the jth component of a known trajectory Y_2, and solve an output tracking problem.

The proposed control strategy is the following. We use the backstepping methodology to map the original augmented system to a simpler target system. Then, we use frequency analysis techniques and some structural assumptions to show that it leads to a control law solving the output regulation-output tracking problem. Inspired by [13,6], we apply filtering techniques to guarantee the delay-robustness of the proposed controller. Next, we solve the problem of state estimation and disturbance reconstruction following a similar approach. We first simplify the system's structure using another backstepping transformation, and then design a Luenberger-like observer for the resulting system. The dynamical output injection gains are obtained through a stability analysis of the error system in the frequency domain. We finally derive an output dynamic feedback ensuring the convergence of the virtual output $\epsilon(t)$ to zero.

2.3 Structural assumptions

The proposed design for our feedback law and state observer requires several sufficient, yet not very restrictive assumptions, that are presented together in this section for simplicity. We also give some insights regarding their conservatism.

Assumption 1 *The boundary couplings ρ, q satisfy $|\rho q| < 1$ and $\rho q \neq 0$.*

This assumption is not overly conservative since, for $|\rho q| > 1$, we would have an infinite number of poles in the closed right half-plane [25,8]. It has been shown in [32] that this, in turn, implies no (delay-)robustness margins in closed-loop. In other words, introducing any arbitrarily small delay in the actuation destabilizes the closed-loop system. Considering the limit case $|\rho q| = 1$ complicates the conditions required for the design and the trade-off does not seem adequate given the focus of this paper. If $\rho = 0$ or $q = 0$, the proposed strategy is not directly applicable but could be easily adapted by slightly modifying the target system, following similar ideas as the ones given in [40]. Moreover, this last condition should not be restrictive from an application perspective since it requires conditions that are unattainable from a practical point of view (e.g., perfect impedance matching between line and load). Finally, it is essential to mention that, as formulated, this assumption can be easily tested and does not require numerical approximations of eigenvalues or eigenfuctions of an infinite-dimensional system.

Assumption 2 *The pairs (A_0, B_0) and (A_{11}, E_1) are stabilizable, i.e. there exist $F_0 \in \mathbb{R}^{p\times n}$, $F_1 \in \mathbb{R}^{1\times m}$ such that $\bar{A}_0 \doteq A_0 + B_0F_0$ and $\bar{A}_{11} \doteq A_{11} + E_1F_1$ are Hurwitz.*

In terms of conservatism, the stabilizability of (A_0, B_0) is only a sufficient condition, yet it allows for a much simpler design of the control law (Section 3.1) as no modes of X need to be stabilized indirectly through the PDE. It is thanks to this conservatism that the condition can be easily tested without need for infinite-dimensional system tools. On the other hand, the second condition on (A_{11}, E_1) is necessary. If not satisfied, the distal ODE system cannot be stabilized.

Assumption 3 *The matrices (A_0, B_0, C_0) satisfy*

$$rank\left(\begin{pmatrix} sI - A_0 & B_0 \\ C_0 & 0_{1\times c} \end{pmatrix}\right) = n + 1, \quad \forall s \in \mathbb{C}, Re(s) \geq 0.$$

This assumption is only sufficient, since some modes of the system could potentially be stabilized through the return signal from the PDE, yet it greatly simplifies the control design and requires no infinite-dimensional tools to check. It implies that C_0 is not identically zero which would have obstructed the stabilization of the system. Also, together with Assumption 2, it guarantees that the function $P_0(s) \doteq C_0(sI - \bar{A}_0)^{-1}B_0$ is stable and does not have any zeros in the right-half complex plane common to all its components. Consequently, $P_0(s)$ admits a (not necessarily proper) stable right-inverse [33]. We denote $P_0^+(s)$ any such right inverse. A possible choice is given by the Moore-Penrose right inverse $P_0^+(s) = P_0^T(s)(P_0(s)P_0^T(s))^{-1}$ (which should be verified to be stable *a posteriori*). If it is not stable, a more involved stable inversion procedure is needed [5].

Assumption 4 *The matrix A_{22} is marginally stable, i.e., all its eigenvalues have zero real parts. For all initial conditions, the zero-input trajectories remain uniformly bounded w.r.t. the norm of the initial condition and in time. Also, there exist matrices $T_a \in \mathbb{R}^{m\times p}$, $F_a \in \mathbb{R}^{1\times p}$ solutions to the* ***regulator equations****:*

$$\begin{cases} -A_{11}T_a + T_aA_{22} + A_{12} = -E_1F_a, \\ -C_{e1}T_a + C_{e2} = 0. \end{cases} \tag{7}$$

This assumption gives a sufficient structural condition for the existence of a solution for the output regulation problem [22]. It can be related to the non-resonance condition. This is a condition on the plant's invariant zeros and the exosystem spectrum at low frequencies. More precisely, A_{11} and A_{22} have disjoint spectra, and the number of outputs we regulate (one in the case of a scalar ϵ) is coherent with c the number of inputs. The matrices T_a, F_a can be easily computed using a Schur triangulation. Once again, the conservatism of this assumption allows the assumption to be checked without requiring infinite-dimensional tools.

We need analogous assumptions to design the proposed state observer.

Assumption 5 *The pairs (A_0, C_{mes}) and (A_1, C_1) are detectable (i.e. there exist $L_X \in \mathbb{R}^{p\times n'}$, $\begin{pmatrix} L_1 & L_2 \end{pmatrix}^T \in \mathbb{R}^{1\times(p+m)}$ such that $A_0^{obs} \doteq A_0 + L_XC_{mes}$ and $A_1^{obs} \doteq A_1 + \begin{pmatrix} L_1 \\ L_2 \end{pmatrix} C_1$ are Hurwitz).*

As before, only the detectability of (A_0, C_{mes}) is necessary, but the one of (A_1, C_1) allows for a simpler observer design.This assumption is sufficient to guarantee the detectability of the interconnected system. Indeed, if all the unobservable states are naturally stable, they do not affect the output feedback controller. We recall that, for the tracking problem, the reference trajectory is assumed to be known.

Assumption 6 *The matrices (A_0, E_0, C_{mes}) satisfy*

$$rank\left(\begin{pmatrix} sI - A_0 & E_0 \\ C_{mes} & 0_{n'\times 1} \end{pmatrix}\right) = n + 1, \quad \forall s \in \mathbb{C}, Re(s) \geq 0.$$

Symmetrically, the column vector E_0 is therefore not identically zero and admits a left inverse. The transfer matrix $P_{\text{mes}}(s) \doteq C_{\text{mes}}(sI - A_0^{\text{obs}})^{-1}E_0$ is stable and has no zeros in the right-half complex plane and admits a stable left-inverse, not necessarily proper.
All assumptions can be easily checked before implementation without the need to solve any kernel equations or otherwise considering the infinite-dimensional nature of the system. It simplifies the use of this methodology for field engineers.

3 State-feedback controller design

In this section, we solve the output tracking-output regulation problem using a state-feedback controller, adjusting the methodology from [13]. The objective is to ensure the convergence to zero of the virtual output $\epsilon(t)$ defined in Section 2.2. First, we use a backstepping transformation to map the initial system to a simpler target system. Next, we use a frequency analysis of this target system to design an adequate feedback controller. Finally, to guarantee the robustness of the resulting control law, we use filtering techniques [6].

3.1 Backstepping transform

Consider integral transform $\mathcal{M} : \mathcal{X} \to \mathcal{X}$, defined by

$$\begin{aligned} X(t) =&\xi(t) + \int_0^1 M^{12}(y)\alpha(t,y) + M^{13}(y)\beta(t,y)\mathrm{d}y \\ &+ \begin{pmatrix} M^{14} & M^{15} \end{pmatrix}\eta(t), \end{aligned} \tag{8}$$

$$Y(t) =\eta(t), \tag{9}$$

$$\begin{aligned} \begin{pmatrix} u(t,x) \\ v(t,x) \end{pmatrix} =& \begin{pmatrix} \alpha(t,x) \\ \beta(t,x) \end{pmatrix} + \int_x^1 \begin{pmatrix} M^{22}(x,y) & M^{23}(x,y) \\ M^{32}(x,y) & M^{33}(x,y) \end{pmatrix} \begin{pmatrix} \alpha(y) \\ \beta(y) \end{pmatrix} \mathrm{d}y \\ &+ \begin{pmatrix} M^{24}(x) & M^{25}(x) \\ M^{34}(x) & M^{35}(x) \end{pmatrix}\eta(t), \end{aligned} \tag{10}$$

with kernel gains and kernel functions $M^{12}, M^{13} \in C([0,1];\mathbb{R}^{n\times 1})$, $M^{14} \in \mathbb{R}^{n\times m}$, $M^{24}, M^{34} \in C([0,1];\mathbb{R}^{1\times m})$ (resp. $M^{15} \in \mathbb{R}^{n\times p}$, $M^{25}, M^{35} \in C([0,1];\mathbb{R}^{1\times p})$), and $M^{22}, M^{23}, M^{32}, M^{33} \in C(\mathcal{T}^+;\mathbb{R})$. This transformation maps the original system (1)-(6) to a target system with a simplified structure. The different kernels satisfy a set of equations given in the following. Since the transform comprises identity operators, integral operators with regular kernels, and products with bounded matrices, it is bounded. This change of variables is therefore well-defined and invertible due to its block triangular structure. The blocks on the diagonal, identity or Volterra integral operator, are all invertible [40,45]. The inverse transform $\mathcal{K} : \mathcal{X} \to \mathcal{X}$, has the same structure

$$\begin{aligned} \xi(t) =&X(t) - \int_0^1 K^{12}(y)u(t,y) + K^{13}(y)v(t,y)\mathrm{d}y \\ &- \begin{pmatrix} K^{14} & K^{15} \end{pmatrix} Y(t), \quad \eta(t) = Y(t), \end{aligned} \tag{11}$$

$$\begin{aligned} \begin{pmatrix} \alpha(t,x) \\ \beta(t,x) \end{pmatrix} =& \begin{pmatrix} u(t,x) \\ v(t,x) \end{pmatrix} - \int_x^1 \begin{pmatrix} K^{22}(x,y) & K^{23}(x,y) \\ K^{32}(x,y) & K^{33}(x,y) \end{pmatrix} \begin{pmatrix} u(y) \\ v(y) \end{pmatrix} \mathrm{d}y \\ &- \begin{pmatrix} K^{24}(x) & K^{25}(x) \\ K^{34}(x) & K^{35}(x) \end{pmatrix} Y(t). \end{aligned} \tag{12}$$

Therein, the coefficients K^{ij} can be expressed in terms of M^{ij} (and reciprocally) [31]

$$\begin{aligned} K^{1i}(x) &= M^{1i}(x) - \textstyle\int_0^x M^{12}(y)K^{2i}(y,x) + M^{13}(y)K^{3i}(y,x)\mathrm{d}y, \\ K^{1j} &= M^{1j} - \textstyle\int_0^1 M^{12}(y)K^{2j}(y) + M^{13}(y)K^{3j}(y)\mathrm{d}y, \\ K^{i'i}(x,y) &= M^{i'i}(x,y) \\ &\quad - \textstyle\int_x^y M^{i'2}(x,\nu)K^{2i}(\nu,y) + M^{i'3}(x,\nu)K^{3i}(\nu,y)\mathrm{d}\nu, \\ K^{ij}(x) &= M^{ij}(x) - \textstyle\int_x^1 M^{i2}(x,y)K^{2j}(y) + M^{i3}(x,y)K^{3j}(y)\mathrm{d}y, \end{aligned}$$

for $i, i' \in \{2,3\}, j \in \{4,5\}$. Using the inverse formulation (8)-(10) simplifies the expression of the coefficients in the target system.

3.2 Target system

Consider transformation $\mathcal{M}$ defined by (8)-(10). We show next that it can map the original system (1)-(6) to the following target system

$$\begin{aligned} \dot{\xi}(t) =& \bar{A}_0\xi(t) - \lambda M^{12}(0)C_0\xi(t) + \bar{E}_1\alpha(t,1) + \bar{E}_0\beta(t,0) \\ &+ \begin{pmatrix} M_1 & M_p \end{pmatrix}\eta(t) + B_0\tilde{U}(t) \\ &+ \int_0^1 M^{\alpha}(y)\alpha(t,y) + M^{\beta}(y)\beta(t,y)\mathrm{d}y, \end{aligned} \tag{13}$$

$$\alpha_t(t,x) + \lambda\alpha_x(t,x) = 0, \quad \beta_t(t,x) - \mu\beta_x(t,x) = 0, \tag{14}$$

$$\dot{\eta}(t) = \begin{pmatrix} \bar{A}_{11} & \bar{A}_{12} \\ 0 & A_{22} \end{pmatrix}\eta(t) + \begin{pmatrix} E_1 \\ 0_{p\times 1} \end{pmatrix}\alpha(t,1), \tag{15}$$

with the boundary conditions

$$\alpha(t,0) = q\beta(t,0) + C_0\xi(t), \quad \beta(t,1) = \rho\alpha(t,1), \tag{16}$$

where $\bar{A}_0, \bar{A}_{11}$ are defined in Assumption 2. Note that the new "unactuated-ODE" state has been decomposed into two parts $\eta(t) = [\eta_1(t)\ \eta_2(t)]^T$. The different coefficients are defined by

$$\begin{aligned} \bar{A}_{12} &= A_{12} + E_1(F_a + F_1T_a), \\ \bar{E}_0 &= E_0 - q\lambda M^{12}(0) + \mu M^{13}(0), \\ \bar{E}_1 &= \lambda M^{12}(1) - M^{14}E_1 - \rho\mu M^{13}(1), \\ M_1 &= -M^{14}\bar{A}_{11} + A_0M^{14} + E_0M^{34}(0), \\ M_p &= -M^{15}A_{22} - M^{14}\bar{A}_{12} + A_0M^{15} + E_0M^{35}(0), \end{aligned}$$

$$M^{\alpha}(y) = -\lambda \frac{\mathrm{d}}{\mathrm{d}y} M^{12}(y) + A_0 M^{12}(y) + E_0 M^{32}(0,y),$$
$$M^{\beta}(y) = \mu \frac{\mathrm{d}}{\mathrm{d}y} M^{13}(y) + A_0 M^{13}(y) + E_0 M^{33}(0,y).$$

The initial condition of this target system is given by $(\xi_0, \alpha_0, \beta_0, \eta_0) = \mathcal{M}(X_0, u_0, v_0, Y_0) \in \mathcal{X}$. Finally, we defined $\tilde{U}(t) \doteq U(t) - F_0\xi(t)$ in (13), with F_0 given in Assumption 2. Without disturbance, this target system was shown to be stabilizable in [13]. This target system presents a cascade structure: the exponential convergence of the state $C_0\xi(t)$ guarantees the regulation of the virtual output $\epsilon(t)$.

3.3 Kernel equations

To map the system (1)-(6) to the target system (13)-(16), we follow the backstepping procedure, yielding the so-called *kernel equations*:

$$\lambda M^{22}_x(x,y) + \lambda M^{22}_y(x,y) = \sigma^+(x) M^{32}(x,y),$$
$$\lambda M^{23}_x(x,y) - \mu M^{23}_y(x,y) = \sigma^+(x) M^{33}(x,y),$$
$$\mu M^{32}_x(x,y) - \lambda M^{32}_y(x,y) = -\sigma^-(x) M^{22}(x,y),$$
$$\mu M^{33}_x(x,y) + \mu M^{33}_y(x,y) = -\sigma^-(x) M^{23}(x,y),$$

with the boundary conditions

$$M^{23}(x,x) = -\frac{\sigma^+(x)}{\lambda+\mu}, \quad M^{32}(x,x) = \frac{\sigma^-(x)}{\lambda+\mu},$$
$$M^{22}(x,1) = \frac{1}{\lambda}\left(M^{24}(x)E_1 + \rho\mu M^{23}(x,1)\right),$$
$$M^{33}(x,1) = \frac{1}{\mu\rho}\left(\lambda M^{32}(x,1) - M^{34}(x)E_1\right).$$

The kernels associated to the state $\eta(t)$ are defined on $[0,1]$ and must satisfy the set of ODEs

$$\lambda \frac{\mathrm{d}}{\mathrm{d}x} M^{24}(x) + M^{24}(x)\bar{A}_{11} = \sigma^+(x) M^{34}(x),$$
$$\lambda \frac{\mathrm{d}}{\mathrm{d}x} M^{25}(x) + M^{25}(x)A_{22} = \sigma^+(x) M^{35}(x) - M^{24}(x)\bar{A}_{12},$$
$$\mu \frac{\mathrm{d}}{\mathrm{d}x} M^{34}(x) - M^{34}(x)\bar{A}_{11} = -\sigma^-(x) M^{24}(x),$$
$$\mu \frac{\mathrm{d}}{\mathrm{d}x} M^{35}(x) - M^{35}(x)A_{22} = -\sigma^-(x) M^{25}(x) + M^{34}(x)\bar{A}_{12},$$

with the boundary conditions

$$M^{24}(1) = F_1, \quad M^{25}(1) = F_a + F_1 T_a,$$
$$M^{34}(1) = C_{11} + \rho F_1, \quad M^{35}(1) = C_{12} + \rho M^{25}(1),$$

where F_1 is defined by Assumption 2 and (F_a, T_a) by Assumption 4. Finally, we also have the following set of algebraic relations

$$C_0 M^{12}(y) = M^{22}(0,y) - qM^{32}(0,y), \tag{17}$$
$$C_0 M^{13}(y) = M^{23}(0,y) - qM^{33}(0,y), \tag{18}$$
$$C_0 M^{14} = M^{24}(0) - qM^{34}(0), \tag{19}$$
$$C_0 M^{15} = M^{25}(0) - qM^{35}(0). \tag{20}$$

We can verify that this set of kernel equations admits a solution. More precisely, we first compute the values of $M^{24}, M^{34} \in C([0,1]; \mathbb{R}^{1\times m})$ and $M^{25}, M^{35} \in C([0,1]; \mathbb{R}^{1\times p})$, using their boundary conditions in $x = 1$ and the coupled ordinary differential equations. Then, using the fact that C_0 is full-row rank, it admits a right-inverse (Moore-Penrose) $C_0^+ \doteq C_0^T(C_0C_0^T)^{-1}$. We can then compute[1] some solution for M^{14}, M^{15}. After these values have been chosen, the set of PDEs is well-posed, and $(M^{22}, M^{23}, M^{32}, M^{33})$ are uniquely defined on their definition domain $\mathcal{C}(\mathcal{T}^+; \mathbb{R})$ [20,26]. Then, we can solve equations (17)-(18) using the Moore-Penrose right-inverse to obtain a specific value for $M^{12}, M^{13} \in C([0,1]; \mathbb{R}^{n\times 1})$.

3.4 Frequency analysis of the target system

Let us denote $\tau = \frac{1}{\mu} + \frac{1}{\lambda}$, the total transport time induced by the transport equations. We now use the method of characteristics to rewrite the target system as a *time-delay system*. The solutions of (14) satisfy, for $t > \tau$, $x \in [0,1]$,

$$\alpha(t,x) = \alpha\left(t - \frac{x}{\lambda}, 0\right), \quad \beta(t,x) = \beta\left(t - \frac{1-x}{\mu}, 1\right). \tag{21}$$

Substituting these expressions in (16), we obtain

$$\alpha(t,0) = \rho q \alpha\left(t-\tau, 0\right) + C_0\xi(t), \tag{22}$$
$$\beta(t,1) = \rho q \beta\left(t-\tau, 1\right) + \rho C_0\xi(t - \frac{1}{\lambda}). \tag{23}$$

In the target system, the transport equations are equivalent to two continuous-time difference equations acting on the boundaries and coupled to the state $\xi(t)$ and to the disturbance $\eta_2(t)$. Taking the Laplace transform of the system (with null initial conditions, we obtain

$$(1 - \rho q \mathrm{e}^{-\tau s})\alpha(s,0) = C_0\xi(s), \tag{24}$$
$$(1 - \rho q \mathrm{e}^{-\tau s})\beta(s,1) = \rho C_0 \mathrm{e}^{-\frac{s}{\lambda}}\xi(s). \tag{25}$$

The Laplace transform of (15) yields

$$(sI - \bar{A}_{11})\eta_1(s) = \bar{A}_{12}\eta_2(s) + E_1 e^{-\frac{s}{\lambda}}\alpha(s,0), \tag{26}$$
$$(sI - A_{22})\eta_2(s) = 0. \tag{27}$$

Multiplying equation (26) by $(1 - \rho q \mathrm{e}^{-\tau s})$,and using (24), we have

$$(1 - \rho q \mathrm{e}^{-\tau s})(sI - \bar{A}_{11})\eta_1(s) = E_1 \mathrm{e}^{-\frac{s}{\lambda}} C_0\xi(s) \tag{28}$$

[1] Even though it seems counterintuitive at first glance, the right-invertibility (and not left invertibility) of C_0 is necessary to solve $C_0X = Y$ (with adequate vectors X, Y). Indeed, since $C_0C_0^+ = Id$, we have $X = C_0^+Y \implies C_0X = C_0C_0^+Y = Y$.

$$+ (1 - \rho q \mathrm{e}^{-\tau s}) \bar{A}_{12} \eta_2(s).$$

Moreover, the matrix polynomial $(sI - \bar{A}_{11})$ is non-singular on the right-half plane from Assumption 2.
Using the delayed equation (21), and a change of variables in the integral terms in (13), we obtain

$$\int_0^1 M^\alpha(y)\alpha(t,y)\mathrm{d}y = \int_0^{\frac{1}{\lambda}} \lambda M^\alpha(\lambda\theta)\alpha(t-\theta,0)\mathrm{d}\theta, \quad (29)$$
$$\int_0^1 M^\beta(y)\beta(t,y)\mathrm{d}y = \int_0^{\frac{1}{\mu}} \mu M^\beta(1-\mu\theta)\beta(t-\theta,1)\mathrm{d}\theta.$$

Consequently, the Laplace transform of (13) becomes

$$\begin{aligned}(sI - \bar{A}_0)\xi(s) &= -\lambda M^{12}(0) C_0\xi(s) + B_0\tilde{U}(s) \quad (30)\\ &+ \left(\bar{E}_1 \mathrm{e}^{-\frac{s}{\lambda}} + \int_0^{\frac{1}{\lambda}} \lambda M^\alpha(\lambda\theta)\mathrm{e}^{-s\theta}\mathrm{d}\theta\right)\alpha(s,0)\\ &+ \left(\bar{E}_0 \mathrm{e}^{-\frac{s}{\mu}} + \int_0^{\frac{1}{\mu}} \mu M^\beta(1-\mu\theta)\mathrm{e}^{-s\theta}\mathrm{d}\theta\right)\beta(.\,,1)(s)\\ &+ M_1\eta_1(s) + M_p\eta_2(s).\end{aligned}$$

Once again, multiplying the quasipolynomial $(1 - \rho q \mathrm{e}^{-\tau s})$ on both sides of (30), and using (24)-(25), we have

$$\begin{aligned}(1 - \rho q \mathrm{e}^{-\tau s})(sI - \bar{A}_0)\xi(s) &= (1 - \rho q \mathrm{e}^{-\tau s})B_0\tilde{U}(s)\\ &- (1 - \rho q \mathrm{e}^{-\tau s})\lambda M^{12}(0)C_0\xi(s)\\ &+ [\bar{E}_1 \mathrm{e}^{-\frac{s}{\lambda}} + \int_0^{\frac{1}{\lambda}} \lambda M^\alpha(\lambda\theta)\mathrm{e}^{-s\theta}\mathrm{d}\theta]C_0\xi(s)\\ &+ [\bar{E}_0 \mathrm{e}^{-\frac{s}{\mu}} + \int_0^{\frac{1}{\mu}} \mu M^\beta(1-\mu\theta)e^{-s\theta}\mathrm{d}\theta]\rho C_0 \mathrm{e}^{-\frac{s}{\lambda}}\xi(s)\\ &+ M_1(sI - \bar{A}_{11})^{-1}E_1 \mathrm{e}^{-\frac{s}{\lambda}} C_0\xi(s)\\ &+ (1 - \rho q \mathrm{e}^{-\tau s})[M_1(sI - \bar{A}_{11})^{-1}\bar{A}_{12} + M_p]\eta_2(s).\end{aligned}$$

Multiplying both sides with $(1-\rho q e^{-\tau s})^{-1}$, we finally obtain for any $s \in \mathbb{C}$ with $\mathrm{Re}(s) \geq 0$

$$(sI - \bar{A}_0)\xi(s) = G(s)C_0\xi(s) + H(s)\eta_2(s) + B_0\tilde{U}(s), \quad (31)$$

with

$$\begin{aligned}G(s) &= -\lambda M^{12}(0) + (1 - \rho q \mathrm{e}^{-\tau s})^{-1}\left[\mathrm{e}^{-\frac{s}{\lambda}}\left(\bar{E}_1\right.\right. \quad (32)\\ &\left.\left. + M_1(sI - \bar{A}_{11})^{-1}E_1\right) + \rho \mathrm{e}^{-\tau s}\bar{E}_0 + \int_0^\tau M^\xi(\theta)\mathrm{e}^{-s\theta}\mathrm{d}\theta\right],\\ M^\xi(\theta) &= \lambda \mathbb{1}_{[0,\frac{1}{\lambda}]}(\theta)M^\alpha(\lambda\theta) \quad (33)\\ &+ \rho\mu \mathbb{1}_{(\frac{1}{\lambda},\tau]}(\theta)M^\beta(1-\mu\theta+\frac{\mu}{\lambda}),\\ H(s) &= M_1(sI - \bar{A}_{11})^{-1}\bar{A}_{12} + M_p. \quad (34)\end{aligned}$$

We now design the function $\tilde{U}(s)$ stabilizing $C_0\xi(s)$ in (31). It, in turn, implies the stabilization of η_1 and ϵ.

3.5 Full-state feedback controller design

Using the superposition principle, the control law is decomposed into two parts: $\tilde{U}(s) = U_\xi(s) + U_\eta(s)$. Using Assumption (2), equation (31) rewrites for any $s \in \mathbb{C}^+$

$$\begin{aligned}C_0\xi(s) &= C_0(sI - \bar{A}_0)^{-1}G(s)C_0\xi(s) + P_0(s)U_\xi(s)\\ &+ C_0(sI - \bar{A}_0)^{-1}H(s)\eta_2(s) + P_0(s)U_\eta(s). \quad (35)\end{aligned}$$

We can use each controller part to compensate for the inner dynamics. First, define the transfer function

$$F_\eta(s) \doteq -P_0^+(s)C_0(sI - \bar{A}_0)^{-1}H(s), \quad (36)$$

such that, knowing the values of η_2, the control law $U_\eta(s) = F_\eta(s)\eta_2(s)$ cancels the effect of the disturbance on the output of the target system. As mentioned above, the obtained transfer function is not proper in general. However, we can use our prior knowledge of the disturbance or trajectory dynamics to regularize it and design a strictly proper transfer function $\tilde{F}_\eta(s)$, following the procedure presented in [5] for instance. We then define

$$\tilde{U}_\eta(s) = \tilde{F}_\eta(s)\eta_2(s). \quad (37)$$

Once we canceled the effects of the disturbance on the dynamics or took into account the given trajectory, equation (35) rewrites

$$C_0\xi(s) = C_0(sI - \bar{A}_0)^{-1}G(s)C_0\xi(s) + P_0(s)U_\xi(s).$$

Next, we define the transfer function

$$F_\xi(s) = -P_0^+C_0(sI - \bar{A}_0)^{-1}G(s) \quad (38)$$

and define $U_\xi(s) = F_\xi(s)C_0\xi(s)$. With this control law, we would obtain $C_0\xi(s) = 0$. However, the transfer function $F_\xi(s)$ may not be strictly proper. Thus, to make it strictly proper and guarantee the existence of robustness margins, we have to use filtering techniques as in [13,6]. Let us decompose $G(s)$ in (32) into $G(s) = \mathrm{w}(s)G(s) + (1 - \mathrm{w}(s))G(s)$, with $\mathrm{w}(s)$ a (SISO) stable low-pass filter of sufficient order, and define a proper transfer function $\tilde{F}_\xi(s)$ by

$$\tilde{F}_\xi(s) = -P_0^+(s)C_0(sI - \bar{A}_0)^{-1}\mathrm{w}(s)G(s) = \mathrm{w}(s)F_\xi(s). \quad (39)$$

We have the following lemma [13]:

Lemma 7 *Let* $\mathrm{w}(s)$ *be any low-pass filter, with a sufficiently high relative degree, and* $0 < \delta < 1$ *sufficiently small, such that*

$$\forall x \in \mathbb{R},\ |1 - \mathrm{w}(jx)| \leq \frac{1-\delta}{\|G\|_\infty \bar{\sigma}(C_0(jxI - \bar{A}_0)^{-1})}. \quad (40)$$

Then the dynamic output feedback $\tilde{U}_\xi(s) + \tilde{U}_\eta(s)$ *with* $\tilde{U}_\xi(s) = \tilde{F}_\xi(s)C_0\xi(s)$ *with* $\tilde{F}_\xi(s)$ *given in* (39)*, and* $\tilde{U}_\eta(s)$ *in* (37) *exponentially stabilizes* $C_0\xi(.)$.

PROOF. First, remark that the relative degree of $\mathrm{w}(s)$ can always be chosen such that $F_\xi(s)$ becomes strictly proper in (39). Once the effects of the trajectory/disturbance have been canceled by $\tilde{U}_\eta(s)$, we can plug (39) into the simplified expression of (35). The closed-loop dynamics of $C_0\xi(.)$ is then governed by $(1-\Phi(s))C_0\xi(s) = 0$, where $\Phi(s) \doteq (1-\mathrm{w}(s))C_0(sI-\bar{A}_0)^{-1}G(s)$. Since $G(s)$ given in (32) is uniformly bounded in the right-half complex plane, we have $\bar{\sigma}(G(jx)) \leq \|G\|_\infty$ for all x. Noting that $\Phi(s)$ is stable and strictly proper ($\bar{A}_0$ is Hurwitz by Assumption 2), we have by (40) that $\bar{\sigma}(\Phi(jx)) \leq 1-\delta$. This implies that $\|\Phi\|_\infty < 1$, which is a sufficient condition for exponential stability of $C_0\xi(.)$. □

We can then define the control input for the original system (1)-(5) as $U(t) = \tilde{U}(t)+F_0\xi(t)$. We now show that the output tracking-output regulation problems are solved.

Theorem 8 *Consider the extended control law*

$$U(s) = (\tilde{F}_\xi(s)C_0 + F_0)\xi(s) + \tilde{F}_\eta(s)\eta_2(s), \qquad (41)$$

where $\tilde{F}_\xi(s), \tilde{F}_\eta(s)$ are two stable strictly proper transfer matrices respectively defined in equations (39) *and* (37)*. Then, under Assumptions 1, 2, 3, 4, the virtual output $\epsilon(t)$ exponentially converges to zero. Furthermore, under the same assumptions, the control action $U(t)$ and the trajectories of X, u, v, and Y remain bounded.*

PROOF. We have already proved in Lemma 7 that $C_0\xi(\cdot)$ is exponentially stabilized by the dynamic output feedback $\tilde{U}_\xi(s) + \tilde{U}_\eta(s) = \tilde{F}_\xi(s)C_0\xi(s) + \tilde{F}_\eta(s)\eta_2(s)$. Due to Assumption 1, $(1-\rho q e^{-\tau s})$ has a stable inverse. Thus, the stability of $\alpha(\cdot,0)$, $\beta(\cdot,1)$ is deduced from (24)-(25), which implies the exponential convergence to zero of α and β in the L^2-norm. Let us now show that $C_{e1}\eta_1 + C_{e2}\eta_2 \longrightarrow 0$. The dynamics of η_1 rewrites

$$\begin{aligned}\dot{\eta}_1(t) &= (A_{11}+E_1F_1)\eta_1(t) + (-E_1F_a + A_{11}T_a - T_aA_{22})\eta_2(t)\\ &\quad + E_1(F_a+F_1T_a)\eta_2(t) + E_1\alpha(t,1) \quad \text{by Assumption 4}\\ &\Longrightarrow \overbrace{(\eta_1+T_a\eta_2)}^{\cdot}(t) = \bar{A}_{11}(\eta_1+T_a\eta_2) + \underbrace{E_1\alpha(t,1)}_{\longrightarrow 0}.\end{aligned}$$

Therefore, the dynamics of $\eta_1 + T_a\eta_2$ are exponentially stable. It implies that $C_{e1}(\eta_1+T_a\eta_2)(t) = C_{e1}(Y_1+T_aY_2)(t) = C_{e1}Y_1(t) + C_{e2}Y_2(t) = \epsilon(t)$ converges to zero. The boundedness of the control input is guaranteed by the fact that functions $\tilde{F}_\xi, \tilde{F}_\eta$ are strictly proper (as $C_0\xi(s)$ exponentially converges to zero and $\eta_2(s)$ is bounded). The boundedness of the state η follows from equation (26). Finally, since $G(s)$ defined by (32) is a stable, proper transfer matrix and since $\bar{A}_0$ is Hurwitz (Assumption 2), we obtain from equation (31) that the state ξ remains bounded. This implies the boundedness of the original state using the invertibility and the boundedness of the backstepping transformation. □

The control law $U(s)$ defined by equation (41) can be expressed in terms of the original coordinates as

$$\begin{aligned}U(s) &= (\tilde{F}_\xi(s)C_0 + F_0)(X(s) - \int_0^1 K^{12}(y)u(s,y)\\ &\quad + K^{13}(y)v(s,y)\mathrm{d}y - \begin{pmatrix}K^{14} & K^{15}\end{pmatrix}Y(s)) + \tilde{F}_\eta(s)Y_2(s).\end{aligned}$$

Thus, its numerical implementation requires a temporal realization of $\tilde{F}_\xi(s)$ in (39) and $\tilde{F}_\eta(s)$ in (37), as well as a numerical approximation of the kernels (11)-(12). Remark that the controller has been chosen as strictly proper which means that it is robust to small delays in the input and parameter uncertainties, which is not the case in some designs that include derivative terms [6]. Finally, this full-state feedback controller requires the knowledge of all the states (X,u,v,Y) at any time, which is not the case in practice. It is then necessary to *estimate* the state (X,u,v,Y_1) and reconstruct the disturbance Y_2 using the available measurement $y(t)$.

4 Dynamic output-feedback controller design

Following a dual approach, we now design a state observer for system (1)-(6). We first use an invertible backstepping transform to map the system to a simpler target system [5], for which the observer design is easier. The proposed Luenberger-like observer is a copy of the target system dynamics with dynamical output injection gains. Using frequency analysis, their tuning guarantees the exponential convergence of the estimated state towards the real one. It is then possible to reconstruct the original state, including the disturbance term. The proposed observer combines the previously designed control law to obtain an output-feedback controller.

4.1 Observer design

4.1.1 Invertible transform and target system

Denote the target system state $(\chi, w, \upsilon, \Omega) \in \mathcal{X}$, where $\Omega(t) = \begin{pmatrix}\Omega_1(t) \mid \Omega_2(t)\end{pmatrix}^T$ is decomposed into two parts. This new state is related to the original one by the following backstepping transform, using the indirect formulation

$$X(t) = \chi(t), \qquad (42)$$

$$\begin{pmatrix}u(t,x)\\ v(t,x)\end{pmatrix} = \begin{pmatrix}w(t,x)\\ \upsilon(t,x)\end{pmatrix} + \int_0^x \begin{pmatrix}L^{22}(x,y) & L^{23}(x,y)\\ L^{32}(x,y) & L^{33}(x,y)\end{pmatrix}\begin{pmatrix}w(y)\\ \upsilon(y)\end{pmatrix}\mathrm{d}y,$$

$$Y(t) = \Omega(t) + \int_0^1 \begin{pmatrix}L^{42}(y)\\ L^{52}(y)\end{pmatrix}w(y) + \begin{pmatrix}L^{43}(y)\\ L^{53}(y)\end{pmatrix}\upsilon(y)\mathrm{d}y. \qquad (43)$$

This transformation, denoted $\mathcal{L}_{\mathrm{obs}}$, is invertible for the same reasons as the transformation $\mathcal{M}$ in Section 3.1. Its inverse transformation is denoted $\mathcal{N}_{\mathrm{obs}}$. The kernel functions $L^{i2}, L^{i3} \in C([0,1];\mathbb{R}^{*\times 1})$ ($* = m$ if $i = 4$, $* = p$ if $i = 5$)

and $L^{22}, L^{23}, L^{32}, L^{33} \in C(\mathcal{T}^-;\mathbb{R})$ are defined in the next subsection.
Following the backstepping methodology, we aim to map the original system to this new target system

$$\dot{\chi}(t) = A_0\chi(t) + E_0\upsilon(t,0) + B_0U(t), \tag{44}$$
$$w_t(t,x) + \lambda w_x(t,x) = g_w(x)\upsilon(t,0) + h_w(x)\chi(t), \tag{45}$$
$$\upsilon_t(t,x) - \mu\upsilon_x(t,x) = g_\upsilon(x)\upsilon(t,0) + h_\upsilon(x)\chi(t), \tag{46}$$
$$\dot{\Omega}(t) = A_1^{\text{obs}}\Omega(t) + K_\Omega^{\upsilon,0}\upsilon(t,0) + K_\Omega^{\chi}\chi(t), \tag{47}$$

with the boundary conditions

$$w(t,0) = q\upsilon(t,0) + C_0\chi(t), \tag{48}$$
$$\upsilon(t,1) = \rho w(t,1) + C_1\Omega(t), \tag{49}$$

with A_1^{obs} defined by Assumption 5. The functions g_w, g_υ and h_w, h_υ satisfy the well-posed set[2] of Volterra integral equations [45]

$$\begin{pmatrix} g_w(x) \\ g_\upsilon(x) \end{pmatrix} + \int_0^x \begin{pmatrix} L^{22}(x,y) & L^{23}(x,y) \\ L^{32}(x,y) & L^{33}(x,y) \end{pmatrix} \begin{pmatrix} g_w(y) \\ g_\upsilon(y) \end{pmatrix} \mathrm{d}y = \mu \begin{pmatrix} L^{23}(x,0) \\ L^{33}(x,0) \end{pmatrix} - \lambda q \begin{pmatrix} L^{22}(x,0) \\ L^{32}(x,0) \end{pmatrix},$$
$$\begin{pmatrix} h_w(x) \\ h_\upsilon(x) \end{pmatrix} + \int_0^x \begin{pmatrix} L^{22}(x,y) & L^{23}(x,y) \\ L^{32}(x,y) & L^{33}(x,y) \end{pmatrix} \begin{pmatrix} h_w(y) \\ h_\upsilon(y) \end{pmatrix} \mathrm{d}y = -\lambda \begin{pmatrix} L^{22}(x,0)C_0 \\ L^{32}(x,0)C_0 \end{pmatrix}.$$

They are uniquely defined on $[0,1]$. The terms $K_\Omega^{\upsilon,0}, K_\Omega^{\chi}$ are then given by

$$K_\Omega^{\upsilon,0} = \mu \begin{pmatrix} L^{43}(0) \\ L^{53}(0) \end{pmatrix} - \lambda q \begin{pmatrix} L^{42}(0) \\ L^{52}(0) \end{pmatrix} - \int_0^1 \begin{pmatrix} L^{42}(y) & L^{43}(y) \\ L^{52}(y) & L^{53}(y) \end{pmatrix} \begin{pmatrix} g_w(y) \\ g_\upsilon(y) \end{pmatrix} \mathrm{d}y,$$
$$K_\Omega^{\chi} = -\lambda \begin{pmatrix} L^{42}(0)C_0 \\ L^{52}(0)C_0 \end{pmatrix} - \int_0^1 \begin{pmatrix} L^{42}(y) & L^{43}(y) \\ L^{52}(y) & L^{53}(y) \end{pmatrix} \begin{pmatrix} h_w(y) \\ h_\upsilon(y) \end{pmatrix} \mathrm{d}y.$$

4.1.2 Kernel equations

To find the equations satisfied by the kernels L^{ij} on their definition domain, we derive equations (44)-(47) with respect to space and time and integrate by parts. Kernels $L^{22}, L^{23}, L^{32}, L^{33}$ satisfy the following set of PDEs

$$\begin{aligned} &\lambda L_x^{22}(x,y) + \lambda L_y^{22}(x,y) = \sigma^+(x)L^{32}(x,y), \\ &\lambda L_x^{23}(x,y) - \mu L_y^{23}(x,y) = \sigma^+(x)L^{33}(x,y), \\ &\mu L_x^{32}(x,y) - \lambda L_y^{32}(x,y) = -\sigma^-(x)L^{22}(x,y), \\ &\mu L_x^{33}(x,y) + \mu L_y^{33}(x,y) = -\sigma^-(x)L^{23}(x,y), \end{aligned} \tag{50}$$

with the boundary conditions

$$\begin{aligned} &L^{23}(x,x) = \frac{\sigma^+(x)}{\lambda+\mu}, \quad L^{32}(x,x) = -\frac{\sigma^-(x)}{\lambda+\mu}, \\ &L^{22}(1,y) = \frac{1}{\rho}(L^{32}(1,y) - C_1\left(L^{42}(y)|L^{52}(y)\right)^T), \\ &L^{33}(1,y) = \rho L^{23}(1,y) + C_1\left(L^{43}(y)|L^{53}(y)\right)^T. \end{aligned}$$

The equations in Ω imply that $L^{42}, L^{43}, L^{52}, L^{53}$ satisfy the following set of ODEs

$$\lambda\frac{\mathrm{d}}{\mathrm{d}y}\begin{pmatrix} L^{42} \\ L^{52} \end{pmatrix}(y) = \begin{pmatrix} A_{11} & A_{12} \\ 0_{p\times m} & A_{22} \end{pmatrix}\begin{pmatrix} L^{42} \\ L^{52} \end{pmatrix}(y) + \begin{pmatrix} E_1 \\ 0_{p\times 1} \end{pmatrix}L^{22}(1,y),$$
$$-\mu\frac{\mathrm{d}}{\mathrm{d}y}\begin{pmatrix} L^{43} \\ L^{53} \end{pmatrix}(y) = \begin{pmatrix} A_{11} & A_{12} \\ 0_{p\times m} & A_{22} \end{pmatrix}\begin{pmatrix} L^{43} \\ L^{53} \end{pmatrix}(y) + \begin{pmatrix} E_1 \\ 0_{p\times 1} \end{pmatrix}L^{23}(1,y),$$

with the boundary conditions

$$\begin{pmatrix} L^{42}(1) \\ L^{52}(1) \end{pmatrix} = -\frac{1}{\lambda}(\rho\begin{pmatrix} L_1 \\ L_2 \end{pmatrix} + \begin{pmatrix} E_1 \\ 0_{p\times 1} \end{pmatrix}), \quad \begin{pmatrix} L^{43}(1) \\ L^{53}(1) \end{pmatrix} = -\frac{1}{\mu}\begin{pmatrix} L_1 \\ L_2 \end{pmatrix}, \tag{51}$$

where the matrices L_1 and L_2 are defined in Assumption 5. To show that this set of kernel equations admits a unique solution, we can adjust the proof from [20], which states the existence of a solution for a general class of kernel equations. The kernels $L^{42}, L^{43}, L^{52}, L^{53}$ can be *embedded* onto the triangular domain $\mathcal{T}^+$, by defining $\tilde{L}^{ij}(x,y) \doteq \mathbb{1}_{x=1}(x,y)L^{ij}(x)$, $i \in \{2,3\}$, $j \in \{4,5\}$. Following [20], we conclude that this system admits a unique bounded solution.

4.1.3 Observer and error state

Using the measurement $y(t) = C_{\text{mes}}X(t) = C_{\text{mes}}\chi(t) \in \mathbb{R}^{n'}$, we now design an observer for the target system. The observer state $(\hat{\chi}, \hat{w}, \hat{\upsilon}, \hat{\Omega})$ is the solution of a set of equations that is a copy of the original dynamics, to which we add dynamical output injection gains $\mathcal{P}$ whose structure is given later[3]. The observer equations are

$$\dot{\hat{\chi}}(t) = A_0\hat{\chi}(t) + E_0\hat{\upsilon}(t,0) + B_0U(t) \tag{52}$$

[2] Note that an explicit expression of g_w, g_υ could have been obtained using the transform $\mathcal{L}_{\text{obs}}$ with the direct formulation. However, it would have led to more complex terms in the boundary conditions (48)-(49).

[3] The observer gains we define do not exactly correspond to the one in the usual Luenberger observer formulation. They do not correspond to static gains, and giving their explicit expression in time is difficult. We use frequency analysis to determine their expression in the Laplace domain.

$$
\begin{aligned}
&\qquad - P_\chi\left(y(t) - C_{\text{mes}}\hat{\chi}(t)\right),\\
&\hat{w}_t + \lambda\hat{w}_x = g_w(x)\hat{v}(t,0) + h_w(x)\hat{\chi}(t) - \mathcal{P}_w(t,x),\\
&\hat{v}_t - \mu\hat{v}_x = g_v(x)\hat{v}(t,0) + h_v(x)\hat{\chi}(t) - \mathcal{P}_v(t,x),\\
&\dot{\hat{\Omega}}(t) = A_1^{\text{obs}}\hat{\Omega}(t) + K_\Omega^{v,0}\hat{v}(t,0) + K_\Omega^{\chi}\hat{\chi}(t) - \mathcal{P}_\Omega(t),
\end{aligned}
$$

with boundary conditions

$$
\begin{aligned}
\hat{w}(t,0) &= q\hat{v}(t,0) + C_0\hat{\chi}(t) - \mathcal{P}_w^0(t),\\
\hat{v}(t,1) &= \rho\hat{w}(t,1) + C_1\hat{\Omega}(t).
\end{aligned} \tag{53}
$$

Initial conditions are arbitrarily chosen in $\mathcal{X}$. The corresponding error state is defined by $(\tilde{\chi},\tilde{w},\tilde{v},\tilde{\Omega}) \doteq (\chi,w,v,\Omega) - (\hat{\chi},\hat{w},\hat{v},\hat{\Omega})$. It satisfies

$$\dot{\tilde{\chi}}(t) = A_0\tilde{\chi}(t) + E_0\tilde{v}(t,0) + P_\chi C_{\text{mes}}\tilde{\chi}(t), \tag{54}$$

$$\tilde{w}_t(t,x) + \lambda\tilde{w}_x(t,x) = g_w(x)\tilde{v}(t,0) + h_w(x)\tilde{\chi}(t) + \mathcal{P}_w(t,x), \tag{55}$$

$$\tilde{v}_t(t,x) - \mu\tilde{v}_x(t,x) = g_v(x)\tilde{v}(t,0) + h_v(x)\tilde{\chi}(t) + \mathcal{P}_v(t,x), \tag{56}$$

$$\dot{\tilde{\Omega}}(t) = A_1^{\text{obs}}\tilde{\Omega}(t) + K_\Omega^{v,0}\tilde{v}(t,0) + K_\Omega^{\chi}\tilde{\chi}(t) + \mathcal{P}_\Omega(t), \tag{57}$$

with the boundary conditions

$$\tilde{w}(t,0) = q\tilde{v}(t,0) + C_0\tilde{\chi}(t) + \mathcal{P}_w^0(t), \tag{58}$$

$$\tilde{v}(t,1) = \rho\tilde{w}(t,1) + C_1\tilde{\Omega}(t). \tag{59}$$

First, we can choose $P_\chi = L_X$, with L_X given in Assumption 5), such that (54) rewrites $\dot{\tilde{\chi}}(t) = A_0^{\text{obs}}\tilde{\chi}(t) + E_0\tilde{v}(t,0)$.

4.1.4 Frequency analysis of the error system

Our objective is now to design the injected signals $\mathcal{P}_w,\mathcal{P}_v,\mathcal{P}_\Omega,\mathcal{P}_w^0$ stabilizing the error system (54)-(59) in the sense of the $\mathcal{X}-$norm. We follow an approach similar to the one given in Section 3.4.

With the chosen P_χ and since $sI - A_0^{\text{obs}}$ is non-singular on the complex right-half plane (Assumption 5), the Laplace transform of (54) gives

$$(sI - A_0^{\text{obs}})\tilde{\chi}(s) = E_0\tilde{v}(s,0) \tag{60}$$

$$\implies \tilde{\chi}(s) = (sI - A_0^{\text{obs}})^{-1}E_0\tilde{v}(s,0) \quad \forall s \in \mathbb{C}^+. \tag{61}$$

Consider the function $P_{\text{mes}}(s)$ defined after Assumption 6, and denote $P_{\text{mes}}^-(s)$ any stable left-inverse. Note that it can be computed using the Hermite normal form or the procedure presented in [5]. Equation (61) implies that $P_{\text{mes}}^- C_{\text{mes}}\tilde{\chi}(s) = \tilde{v}(s,0)$.

Let us now focus on equations (55)-(56). We want to choose signals $\mathcal{P}_w,\mathcal{P}_v$ to suppress the in-domain couplings, such that the two PDEs rewrite as pure transport equations. It implies that $\tilde{w}(t,x) \equiv \tilde{w}(t-\frac{x}{\lambda},0)$, $\tilde{v}(t,x) \equiv \tilde{v}(t-\frac{1-x}{\mu},1)$ or, in the frequency domain, $\tilde{w}(s,1) \equiv e^{-\frac{s}{\lambda}}\tilde{w}(s,0)(s)$, $\tilde{v}(s,0) \equiv e^{-\frac{s}{\mu}}\tilde{v}(s,1)$. Applying the method of characteristics to system (55)-(56), we have

$$
\begin{aligned}
\tilde{w}(t,1) =& \tilde{w}(t-\frac{1}{\lambda},1) + \int_0^{\frac{1}{\lambda}} g_w(1-\lambda\theta)\tilde{v}(t-\theta,0) \\
&+ h_w(1-\lambda\theta)\tilde{\chi}(t-\theta) + \mathcal{P}_w(t-\theta,1-\lambda\theta)\mathrm{d}\theta,
\end{aligned} \tag{62}
$$

$$
\begin{aligned}
\tilde{v}(t,0) =& \tilde{v}(t-\frac{1}{\mu},0) + \int_0^{\frac{1}{\mu}} g_v(\mu\theta)\tilde{v}(t-\theta,0) \\
&+ h_v(\mu\theta)\tilde{\chi}(t-\theta) + \mathcal{P}_v(t-\theta,\mu\theta)\mathrm{d}\theta.
\end{aligned} \tag{63}
$$

Taking the Laplace transform of (62)-(63), and incorporating (61), we have

$$
\begin{aligned}
&\tilde{w}(s,1) = e^{-\frac{s}{\lambda}}\tilde{w}(s,0) + \int_0^{\frac{1}{\lambda}} (g_w(1-\lambda\theta) + h_w(1-\lambda\theta) \\
&(sI - A_0^{\text{obs}})^{-1}E_0)\tilde{v}(s,0)(s) + \mathcal{P}_w(s,1-\lambda\theta))e^{-s\theta}\mathrm{d}\theta.
\end{aligned} \tag{64}
$$

$$
\begin{aligned}
&\tilde{v}(s,0) = e^{-\frac{s}{\mu}}\tilde{v}(s,1) + \int_0^{\frac{1}{\mu}} (g_v(\mu\theta) \\
&+ h_v(\mu\theta)(sI - A_0^{\text{obs}})^{-1}E_0)\tilde{v}(s,0) + \mathcal{P}_v(s,\mu\theta))e^{-s\theta}\mathrm{d}\theta.
\end{aligned} \tag{65}
$$

We now consider that we have gains of the form $\mathcal{P}_w(s,x) = P_w(s,x)C_{\text{mes}}\tilde{\chi}(s)$, $\mathcal{P}_v(s,x) = P_v(s,x)C_{\text{mes}}\tilde{\chi}(s)$, which only depend on the available measurement and the observer state. To cancel the terms in the integral, we thus define the transfer functions

$$P_w(s,x) \doteq -(g_w(x) + h_w(x)(sI - A_0^{\text{obs}})^{-1}E_0)P_{\text{mes}}^-(s). \tag{66}$$

$$P_v(s,x) \doteq -(g_v(x) + h_v(x)(sI - A_0^{\text{obs}})^{-1}E_0)P_{\text{mes}}^-(s). \tag{67}$$

Let us now consider the boundary condition (58). Taking its Laplace transform and incorporating therein (61), we have

$$\tilde{w}(s,0) = (q + C_0(sI - A_0^{\text{obs}})^{-1}E_0)\tilde{v}(s,0) + \mathcal{P}_w^0(s).$$

Choosing $\mathcal{P}_w^0(s) \doteq P_w^0(s)C_{\text{mes}}\tilde{\chi}(s)$, we define

$$P_w^0(s) \doteq -(q + C_0(sI - A_0^{\text{obs}})^{-1}E_0)P_{\text{mes}}^-(s), \tag{68}$$

such that the reflection terms at the boundary are cancelled[4]. Finally, taking the Laplace transform of (57) and incorporating therein (61), we have

$$
\begin{aligned}
(sI - A_1^{\text{obs}})\Omega(s) = (K_\Omega^{v,0} + K_\Omega^{\chi}(sI - A_0^{\text{obs}})^{-1}E_0)\tilde{v}(s,0) \\
+ \mathcal{P}_\Omega(s),
\end{aligned}
$$

with $sI - A_1^{\text{obs}}$ non-singular on $\mathbb{C}^+$ by Assumption 5. With an input signal of form $\mathcal{P}_\Omega(s) = P_\Omega(s)C_{\text{mes}}\tilde{\chi}(s)$, the transfer

[4] Although canceling boundary reflection terms can have negative effects on robustness margins [4], the use of an adequate low-pass filter does not, however, prevent the output feedback control law from being robust with regard to small delays [6].

function

$$P_\Omega(s) = \quad -(K_\Omega^{\upsilon,0} + K_\Omega^{\chi}(sI - A_0^{\text{obs}})^{-1}E_0)P_{\text{mes}}^{-}(s), \quad (69)$$

guarantees the convergence of $\tilde{\Omega}$ to zero. Finally, we can use a low-pass filter $\omega(s)$ to ensure all the transfer functions defining the observer gains are strictly proper

$$\mathcal{P}_w(s,x) = \omega(s)P_w(s,x)C_{\text{mes}}\tilde{\chi}(s), \quad (70)$$
$$\mathcal{P}_\upsilon(s,x) = \omega(s)P_\upsilon(s,x)C_{\text{mes}}\tilde{\chi}(s), \quad (71)$$
$$\mathcal{P}_\Omega(s) = \omega(s)P_\Omega(s)C_{\text{mes}}\tilde{\chi}(s), \quad (72)$$
$$\mathcal{P}_w^0(s) = \omega(s)P_w^0(s)C_{\text{mes}}\tilde{\chi}(s). \quad (73)$$

The exponential stability of the error system is stated in the following theorem

Theorem 9 *Let $\omega(s)$ be any low pass filter with a sufficiently high relative degree, and $0 < \tilde{\delta} < 1$ sufficiently small, such that*

$$\forall x \in \mathbb{R}, |1 - \omega(jx)| < \frac{1-\tilde{\delta}}{|\rho q| + \bar{\sigma}(G_{obs}(jx))}, \quad (74)$$

with

$$G_{obs}(s) \doteq \rho \left[e^{-\tau s}C_0(sI - A_0^{obs})^{-1} + e^{-\frac{s}{\mu}} \times \right. \quad (75)$$
$$\left. \int_0^{\frac{1}{\lambda}} \left(g_w(1-\lambda\theta) + h_w(1-\lambda\theta)(sI - A_0^{obs})^{-1}E_0 \right) e^{-s\theta}\mathrm{d}\theta \right]$$
$$+ \int_0^{\frac{1}{\mu}} \left(g_\upsilon(\mu\theta) + h_\upsilon(\mu\theta)(sI - A_0^{obs})^{-1}E_0 \right) e^{-s\theta}\mathrm{d}\theta$$
$$+ C_1(sI - A_1^{obs})^{-1} \left(K_\Omega^{\nu,0} + K_\Omega^{\chi}(sI - A_0^{obs})^{-1}E_0 \right).$$

Consider the dynamic output feedback gains (70)-(73) *with $P_w(s,x)$, $P_\upsilon(s,x)$, $P_\Omega(s)$, $P_w^0(s)$ defined by* (66)-(69)*. Then, under Assumptions 5 and 6, the error system* (54)-(59)*, with any initial conditions in $\mathcal{X}$, is exponentially stable in the sense of the $\mathcal{X}-$norm.*

PROOF. First, we emphasize that we can always find a low pass filter ω and a coefficient $\tilde{\delta}$ such that condition (74) is satisfied. Indeed, the transfer function $G_{\text{obs}}(s)$ is strictly proper and uniformly bounded in the right-half complex plane as a sum of strictly proper transfer functions. The integral term goes to zero at high frequencies by the Riemann-Lebesgue lemma. Thus, at high frequency, $|G_{\text{obs}}(jx)| \longrightarrow 0$ and the gain of the low-pass filter goes to zero $|\omega(jx)| \longrightarrow 0$. Since $|\rho q| < 1$ by Assumption 1, we can choose $0 < \tilde{\delta} < 1 - |\rho q|$. An example of an adequate filter design is proposed in [6]. Plugging (70)-(73) into the Laplace transform of (54)-(59), we obtain

$$\tilde{\chi}(s) = (sI - A_0^{\text{obs}})^{-1}E_0\tilde{\upsilon}(s,0),$$
$$\tilde{w}(s,1) = e^{-\frac{s}{\lambda}}\tilde{w}(s,0) - (1-\omega(s)) \int_0^{\frac{1}{\lambda}} [g_w(1-\lambda\theta)$$
$$+ h_w(1-\lambda\theta)(sI - A_0^{\text{obs}})^{-1}E_0]e^{-s\theta}\mathrm{d}\theta\tilde{\upsilon}(s,0),$$
$$\tilde{\upsilon}(s,0) = e^{-\frac{s}{\mu}}\tilde{\upsilon}(s,1) - (1-\omega(s)) \int_0^{\frac{1}{\mu}} [g_\upsilon(\mu\theta)$$
$$+ h_\upsilon(\mu\theta)(sI - A_0^{\text{obs}})^{-1}E_0]e^{-s\theta}\mathrm{d}\theta\tilde{\upsilon}(s,0),$$
$$(sI - A_1^{\text{obs}})\Omega(s) = (1-\omega(s))[(K_\Omega^{\nu,0}\tilde{\upsilon}(s,0) + K_\Omega^{\chi}\tilde{\chi}(s)],$$
$$\tilde{w}(s,0) = (1-\omega(s))[q\tilde{\upsilon}(s,0) + C_0\tilde{\chi}(s)],$$
$$\upsilon(s,1) = \rho\tilde{w}(s,1) + C_1\Omega(s).$$

Combining the above equations, the closed-loop dynamics of $\tilde{\upsilon}(.,0)$ rewrite

$$\tilde{\upsilon}(s,0) = (1-\omega(s))[\rho q e^{-s\tau} + G_{\text{obs}}(s)]\tilde{\upsilon}(s,0),$$
$$= \Phi_{\text{obs}}(s)\tilde{\upsilon}(s,0), \quad (76)$$

with $G_{\text{obs}}(s)$ defined in (75). Thus, $\Phi_{\text{obs}}(s)$ is stable and strictly proper. We have

$$\bar{\sigma}(\Phi_{\text{obs}}(jx)) \leq |1-\omega(jx)|\ \bar{\sigma}(\rho q e^{-j\tau x} + G_{\text{obs}}(jx))$$
$$< 1 - \tilde{\delta}, \quad \forall x \in \mathbb{R}, \text{ by (74).}$$

This implies that $\|\Phi_{\text{obs}}\|_\infty < 1$, which is a sufficient condition for exponential stability of $\tilde{\upsilon}(.,0)$ in (76). The end of the proof is a consequence of Assumption 5. □

Under Assumption 6, we thus designed dynamical observer gains stabilizing the target error system. Let us now define the original observer state

$$(\hat{X}, \hat{u}, \hat{v}, \hat{Y}) = \mathcal{L}_{\text{obs}}(\hat{\chi}, \hat{w}, \hat{\upsilon}, \hat{\Omega}). \quad (77)$$

We have

Corollary 10 *Let $\omega(s)$ be any low pass filter with a sufficiently high relative degree, satisfying* (74) *and the dynamic output feedback of form* (70)-(73) *with $P_w(s,x), P_\upsilon(s,x), P_\Omega(s)$ and $P_w^0(s)$ defined by* (66)-(69)*. Then, under assumptions 5, and 6, the observer state* (77) *converges towards the original state (X,u,v,Y) exponentially.*

PROOF. Under the corollary assumptions, the target error state converges to zero at an exponential rate by Theorem 11. Consequently, the target observer state converges towards the target state. We, therefore, have access to an estimation of the state $(\chi, w, \upsilon, \Omega)$ with the observer state. Using the invertible backstepping transform $\mathcal{L}_{\text{obs}}$ defined by (42)-(43), we can reconstruct the original state (X,u,v,Y). Indeed, we can define the original error state as $(\tilde{X}, \tilde{u}, \tilde{v}, \tilde{Y}) = (X,u,v,Y) - (\hat{X}, \hat{u}, \hat{v}, \hat{Y})$. Since the backstepping transform is invertible, the original error system shares the same stability properties with the target error system, and is thus exponentially stable. Since the original error state converges to zero, the original observer is a correct estimation of the original state. □

4.2 Output-feedback controller

We can now state the most important result of this paper.

Theorem 11 *Consider system* (1)-(6) *with the observer* (52)-(53)*,* (77) *and the control law*

$$\begin{aligned}\hat{U}(s) =&(\tilde{F}_\xi(s)C_0 + F_0)[\hat{X}(s) - K^{14}\hat{Y}_1(s)\\ &- \int_0^1 K^{12}(y)\hat{u}(s,y) + K^{13}(y)\hat{v}(s,y)\mathrm{d}y]\\ &+ [\tilde{F}_\eta(s) - (\tilde{F}_\xi(s)C_0 + F_0)K^{15}]\hat{Y}_2(s), \qquad (78)\end{aligned}$$

with $\tilde{F}_\xi(t)$ defined by (39) *and $\tilde{F}_\eta(s)$ defined in* (37)*. Then, for all initial conditions $(X_0, u_0, v_0, Y_0) \in \mathcal{X}$, the virtual output $\epsilon(t)$ exponentially converges to zero and the state of the system remains bounded in the $\mathcal{X}-$norm.*

PROOF. Using the previous results, we need to show that the dynamics of $C_0\xi$ are stabilized by the output feedback law (78). By Corollary 10, the error state $(\tilde{X}, \tilde{u}, \tilde{v}, \tilde{Y})$ exponentially converges to zero. Due to the invertibility of the backstepping transform $\mathcal{K}$ defined in (11)-(12), the target error state $(\tilde{\xi}, \tilde{\alpha}, \tilde{\beta}, \tilde{\eta}) = \mathcal{K}(\tilde{X}, \tilde{u}, \tilde{v}, \tilde{Y})$ is exponentially stable. Denote $\mathcal{E}$ the well-defined linear operator such that $\hat{U} = \mathcal{E}(\hat{\xi}, \hat{\alpha}, \hat{\beta}, \hat{\eta}) = \mathcal{E}(\xi, \alpha, \beta, \eta) - \mathcal{E}(\tilde{\xi}, \tilde{\alpha}, \tilde{\beta}, \tilde{\eta})$. The dynamics of ξ and the error state have a cascaded structure. Indeed, from (31), we have

$$\begin{aligned}(sI - \bar{A}_0)\xi(s) = G(s)C_0\xi(s) + H(s)\eta_2(s)\\ + B_0(\hat{U}(s) - F_0\xi(s)),\end{aligned}$$

and then by linearity

$$\underbrace{(sI - \bar{A}_0)\xi(s) = G(s)C_0\xi(s) + H(s)\eta_2(s) + B_0\bar{U}(s)}_{\text{exponentially stable dynamics}}$$
$$\underbrace{-B_0\mathcal{E}(\tilde{\xi}, \tilde{\alpha}, \tilde{\beta}, \tilde{\eta}).}_{\text{autonomous exponentially stable system}}$$

The dynamics of (α, β, η) are not modified, and $C_0\xi$ converges to zero. We can apply the results from Section 3.5 to conclude. □

5 Numerical simulation

In this section, we illustrate the performance of our output feedback controller in two test cases where the original open-loop system is unstable. In the first test case, we consider an industry-inspired example in which the two ODE systems are exponentially stable with a slow convergence rate. Such a situation can appear when modeling the evolution of axial vibrations in drilling devices [3,9]. In this case, the actuator dynamics (ODE X) and the linearized bit-rock interaction law (ODE Y) are exponentially stable. For this application test case, some non-linear dynamics might cause undesired oscillations such as bit-bouncing, which must be neglected here. Although the ODEs are exponentially stable in this first example, the coupling with the PDE can make the interconnected system unstable. The control objective in this test case is to follow a sinusoidal signal in the presence of a constant disturbance. The second test case is an academic example where we fully exploit the weakest form of all assumptions. It is a worst-case scenario, inspired by [13], where all the subsystems are independently unstable, only stabilizable and detectable. The controller has to compensate for all the instabilities in the system. Such pathological test case is chosen on purpose as it does not satisfy the conditions of results found in the literature. The control objective is here to stabilize the system in the presence of a sinusoidal disturbance. For both examples, the system, the observer, and the controller were implemented using Matlab and Simulink. The evolution of the PDE systems was simulated using an explicit in-time, first-order, upwind finite difference method. The ODE states were simulated using a Runge-Kutta solver (order 4) with fixed timesteps. The transfer functions in the control law were transformed into a state-space representation for implementation. The evolution of the systems was computed with a CFL number equal to 0.5.

5.1 First test case: trajectory tracking in the presence of a constant disturbance

Consider system (1)-(6) with the following numerical values: $\lambda = 2$, $\mu = 0.7$, $\sigma^+(x) = 0.5 + 0.1\sin(x)$, $\sigma^- = 0.5$, $\rho = 0.5$, $q = 0.6$. The ODE dynamics are in dimension $n = 4, m = 3, c = 2$, and defined by the matrices

$$A_0 = \begin{pmatrix} 0 & 0.014 & 0 & 0.01 \\ -4.2 & -0.5 & 0 & 0 \\ 0 & 0 & -0.15 & 0.2 \\ 0 & 0 & 0 & -0.11 \end{pmatrix}, B_0 = \begin{pmatrix} 0 & 0 \\ 0 & -1 \\ 1 & -1 \\ 0 & 0 \end{pmatrix}, E_0 = \begin{pmatrix} 0.2 \\ -0.1 \\ 0.01 \\ 0 \end{pmatrix},$$

$$C_0 = \begin{pmatrix} 0.1 & 0 & 0 & -0.05 \end{pmatrix}, \; C_1 = \begin{pmatrix} 0 & 1 & 0.5 & 0.1 & 0 & 0 \end{pmatrix},$$

$$A_{11} = \begin{pmatrix} -0.29 & 0.14 & 0 \\ -0.14 & 0 & 0.1 \\ 0 & 0 & -0.9 \end{pmatrix}, A_{21} = \begin{pmatrix} 0 & 0 & 0 \\ 0 & 0 & 0 \\ 0 & 0 & 0 \end{pmatrix}, A_{12} = \begin{pmatrix} 1 & 0 & 0 \\ 0 & 0 & 0 \\ 0 & 0 & 0 \end{pmatrix},$$

$$A_{22} = \begin{pmatrix} 0 & 0 & 0 \\ 0 & 0 & 1 \\ 0 & -1 & 0 \end{pmatrix}, E_1 = \begin{pmatrix} -0.1 \\ -0.1 \\ 0 \end{pmatrix}.$$

With this choice of coefficients, the two ODE subsystems are independently exponentially stable as A_0 and A_1 are Hurwitz. However, the interconnection with the PDE makes the interconnection unstable, as seen in Figure 2. With this choice of matrices, the exogenous state has the following

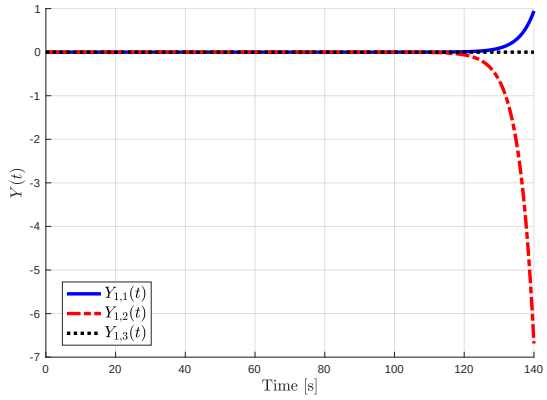

Fig. 2. Evolution of the distal ODE state $Y_1(t)$ in open-loop for the first test case (divided by 10^{10}).

dynamics

$$\dot{Y}_2(t) = A_{22}Y_2(t), \text{ with } Y = \begin{pmatrix} Y_{\text{pert}} & Y_{\text{ref}} & \dot{Y}_{\text{ref}} \end{pmatrix}^\top.$$

The constant disturbance acts on the first component of $Y_1(t)$ and the right boundary of the PDE system. The virtual input is defined by $\epsilon(t) = Y_{1,1}(t) - Y_{\text{ref}}(t)$, which gives $C_e = \begin{pmatrix} 1 & 0 & 0 & -1 & 0 & 0 \end{pmatrix}$, that is, we want the first component of Y_1 to track the reference sinusoidal signal. We can easily verify that the different assumptions are satisfied. The control kernels M^{ij}, K^{ij} (Section 3) and the observer kernels L^{ij}, N^{ij} (Section 4.1) are computed off-line using a fixed-point algorithm based on the successive approximation technique, with a tolerance of 10^{-7}. The integral terms are numerically approximated by the trapezoidal method. We used a `nx` = 101 points mesh to discretize the space domain. Since the ODEs are naturally exponentially stable in this example, we choose small observer and controller gains to avoid numerical problems. In particular, we choose $F_0 = 0, L_X = 0, F_1 = 0$, and

$$L_1 = \begin{pmatrix} 0 & -0.1 & 0 \end{pmatrix}^\top, \; L_2 = \begin{pmatrix} 0.02 & 0 & 0 \end{pmatrix}^\top.$$

The control input is subject to a 0.1s delay. We used simple low-pass filters of 4th order with different bandwidths as detailed in [6]. The observer is initialized with arbitrary values. The simulations are obtained in less than one minute, and the proposed control strategy guarantees the convergence of the virtual output to zero: as seen in Figure 3, the signal Y_1 converges to the reference signal. Moreover, the corresponding estimations match the real signals. The associated control effort is pictured in Figure 4. Finally, a 3D representation of $v(t,x)$ is given in Figure 3. This signal oscillates in the steady state as expected since the reference signal is a sinusoidal function. Finally, the estimation of the constant disturbance is pictured in Figure 6. This estimated signal does not perfectly converge to the real value but some small oscillations remain. These oscillations are induced by the numerical approximations and may decrease when using a smaller time step. Note that this system remains numerically stiff due to the high bandwidth of the filtered inverse subsystems and the slow components in some of the ODE systems.

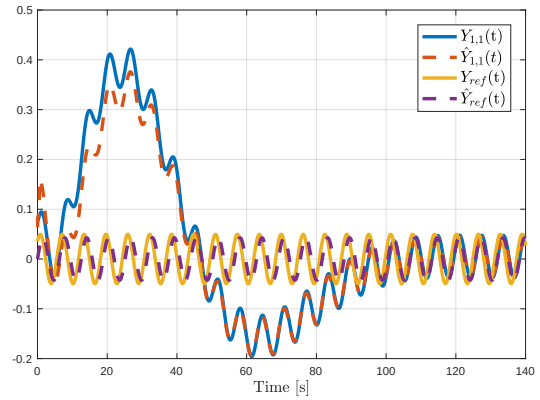

Fig. 3. Evolution of the distal ODE state $Y_{1,1}(t)$ and its estimation in closed-loop for the first test case. The reference signal Y_{ref} and its estimation are also pictured.

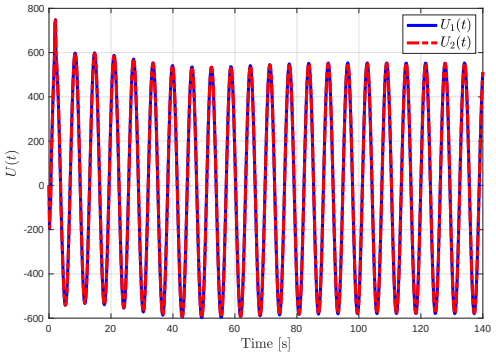

Fig. 4. Evolution of control efforts $U_1(t)$ and $U_2(t)$ for the first test case.

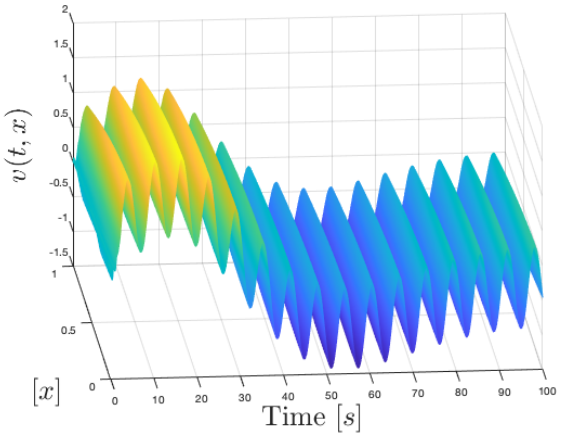

Fig. 5. Evolution of PDE state $v(t,x)$ for the first test case.

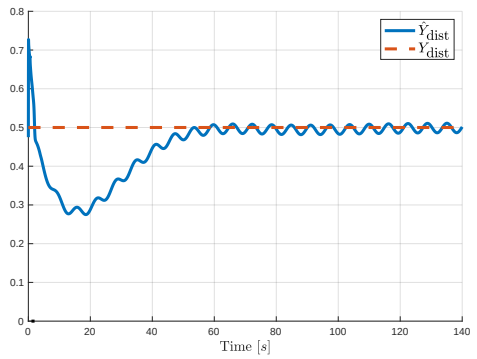

Fig. 6. Evolution of the disturbance signal Y_{dist} and its estimation $\hat{Y}_{\text{dist}}$ in the first test case.

5.2 *Second test case: sinusoidal disturbance rejection for a pathological system*

In this second test case, we consider the disturbance rejection problem for a worst-case scenario. It is an academic example, inspired by [13], that illustrates how the proposed approach fully exploits the weakest form of all assumptions. Consider system (1)-(6) with the following numerical values: $\lambda = 2$, $\mu = 0.7$, $\sigma^+ = 0.3$, $\sigma^- = 0.2$, $\rho = 0.5$, $q = 0.6$. The in-domain coupling terms are constant to reduce the computational effort, which is already very important. The ODE dynamics are in dimension $n = 4, m = 3, p = 3$, and defined by the matrices

$$A_0 = \begin{pmatrix} 0 & 0.14 & 0 & 0.1 \\ 0 & 0 & 0.14 & 0 \\ 0.29 & -0.43 & 0.57 & 0.2 \\ 0 & 0 & 0 & -1.1 \end{pmatrix}, B_0 = \begin{pmatrix} 0 & 0 \\ 0 & -1 \\ 1 & -1 \\ 0 & 0 \end{pmatrix}, E_0 = \begin{pmatrix} 2 \\ -1 \\ 0.1 \\ 0 \end{pmatrix},$$

$$C_0 = \begin{pmatrix} 1 & 0 & 0 & -0.5 \end{pmatrix}, C_{11} = \begin{pmatrix} 3 & -0.6 & 0 \end{pmatrix},$$

$$A_{11} = \begin{pmatrix} 0.1 & 0 & 0 \\ 0.05 & -0.1 & -0.02 \\ 0 & 0 & -0.2 \end{pmatrix}, E_1 = \begin{pmatrix} 0.1 \\ -0.05 \\ 0 \end{pmatrix}.$$

The exogenous system is a sinusoidal signal that verifies

$$\dot{Y}_2(t) = A_{22} Y_2(t) = \begin{pmatrix} 0 & \pi \\ -\pi & 0 \end{pmatrix} Y_2(t).$$

The exogenous signal only acts on the Y-ODE subsystem (i.e., $C_{12} = [0, 0]$) through the matrix A_{12} defined by

$$A_{12} = \begin{pmatrix} 0 & 0.2 & 0.05 \\ 0.1 & 0 & 0 \end{pmatrix}^T.$$

The virtual input is defined by $C_e = \begin{pmatrix} 1 & 0 & 0 & 0 & 0 \end{pmatrix}$, such that $\epsilon(t) = Y_{1,1}(t)$. Thus, the control objective is to stabilize the first component of $Y_1(t)$ in the presence of an exogenous sinusoidal disturbance. This second test case can be considered as a worst-case scenario since all the subsystems are independently unstable, only stabilizable or detectable. However, we can verify that the different assumptions are satisfied. Notice in particular that $A_{12} \notin Im(E_1)$ (unmatched disturbance), $C_0 B_0 = 0$, $E_0 \notin Im(B_0)$ and (A_0, B_0) is not controllable but is stabilizable. We chose the same system as in [13] since it has the right properties to illustrate the assumptions in the paper (detectability, stabilizability, unstable system, unmatched disturbances, etc.) while having a reasonable complexity and order. As illustrated in Figure 7, the norm of the unstable open-loop system explodes. To design the observer and the output-feedback control law, we used the following set of coefficients

$$F_0 = \begin{pmatrix} 41.71 & 5.43 & -1.93 & 0 \\ 42 & 5 & 0.14 & 0 \end{pmatrix}, F_1 = \begin{pmatrix} -5 & -15 & 0 \end{pmatrix},$$

$$L_X = \begin{pmatrix} -2.45 & -0.21 \\ -0.22 & -3.49 \\ -15.34 & 187.6 \\ -129.5 & 20.2 \end{pmatrix}, L_1 = \begin{pmatrix} -0.72 \\ 0 \\ -0.1 \end{pmatrix}, L_2 = \begin{pmatrix} -21.2 \\ 27.9 \end{pmatrix},$$

and $L_Y = \begin{pmatrix} -0.72 & 0 & -0.1 & -21.1 & 27.9 \end{pmatrix}^T$. The control and observer kernels are computed off-line using as in the previous example, but with a reduced space step of 0.0025. It implies that the computational time required to simulate the system is much larger. Then, the system under consideration is numerically very stiff and takes an important effort to simulate. We used simple low-pass filters of 4th order with different bandwidths as detailed in [6]. The observer is initialized with values corresponding to 60% of the real values. The system is subject to a 10ms input delay, corresponding to about 10 time steps. Although this input delay is small, it is large enough to be distinguished from numerical artifacts. To avoid numerical issues with a larger delay, we would need a smaller time step, and consequently, the simulations would require a longer computation time. Due to the large computational cost of running these simulations, we did not consider higher delay values. Moreover, we recall that our theoretical result is the existence of a non-zero delay margin and not its explicit characterization. As shown in Figure 8, the virtual output $\epsilon(t)$ converges to zero with the output-feedback control law, even in the presence of the disturbance signal. The control objective is therefore fulfilled.

The control inputs are pictured in Figure 9 and the evolution of the PDE state $v(t, x)$ in Figure 10. This state remains bounded. The controller takes very large values, compared to the first test case, since it has to compensate for all the system's instabilities (particularly those in the distal ODE system). The delay margin is non-zero but might be small in this highly unstable case. As seen previously, we can expect better simulation behavior and delay margins for less unstable systems. In a practical application, as for a heavy

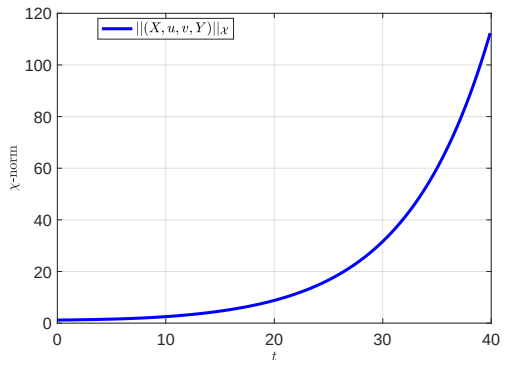

Fig. 7. Evolution of the $\mathcal{X}$-norm in open-loop for the second test case.

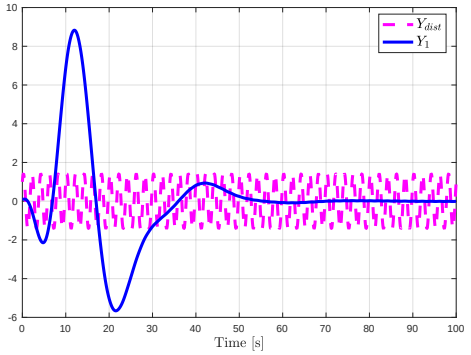

Fig. 8. Evolution of the distal ODE state $Y_1(t)$ (blue) for the second test case, in the presence of a disturbance Y_{dist} (dotted pink).

industrial system, we would not expect all of the components of the interconnected system to be independently unstable and simply stabilizable. In particular, the PDE would most likely be destabilized by the interconnection with the ODE and not by itself, and the actuator would not be an unstable ODE. The actuation will then likely require a lot less energy. Furthermore, we would expect a slow system with a smaller bandwidth to have a higher delay margin naturally. Optimizing the filter could increase the delay margin, yet, without a theoretical bound for this, it is outside of the scope of this paper.

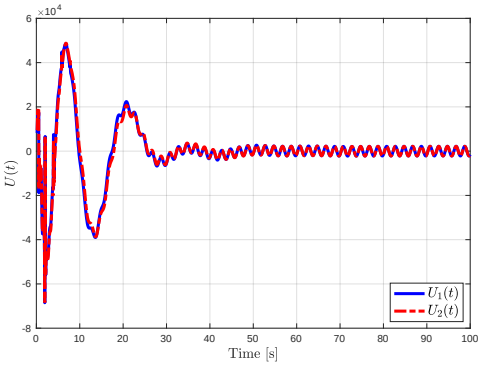

Fig. 9. Evolution of the control inputs $U_1(t)$ (blue) and $U_2(t)$ (red) for the second test case.

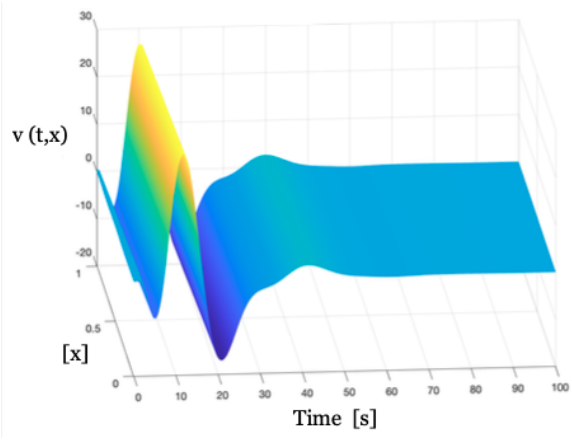

Fig. 10. Evolution of the PDE state $v(t,x)$ for the second test case.

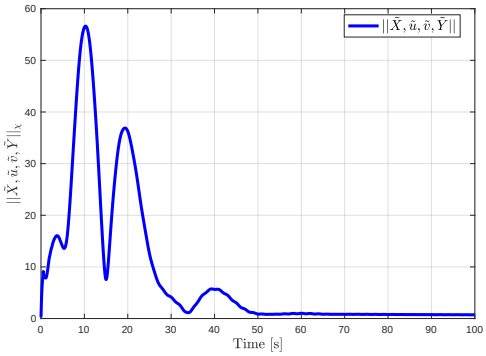

Fig. 11. Evolution of the $\mathcal{X}-$norm of the error state for the second test case.

Finally, the evolution of the norm of the error state is represented in Figure 11. As expected, the error seems to converge to zero after the transient. However, the final value is not precisely zero. Even if this discrepancy does not prevent the stabilization of the virtual output in a closed loop, it means that some of our states are not correctly reconstructed. This mismatch is due mainly to numerical issues since we noticed that reducing the space step, and consequently the time step, implied getting better estimates. Indeed, when performing the backstepping transformations, some kernels or some states may have large values compared to others, which could explain the sensitivity when performing the change of coordinates. Reducing the space step may slow the computations, which is a problem in a real implementation. It could be interesting to consider implicit solvers or use the Simpson method to compute the different integral terms instead of the trapezoidal method to overcome this numerical problem, which is currently a limitation to the proposed approach. Finally, it is essential to mention that this numerical issue occurs because of the strong instability of the open-loop system chosen as an example. Once again, the second simulation scenario was selected on purpose, not as a "nice" case, but one that does not satisfy the conditions of previous results in the literature.

6 Notes, comments and concluding remarks

In this paper, we designed a strictly proper dynamic output-feedback controller to solve the output regulation and output tracking problem for a class of interconnected ODE-PDE-ODE systems. The load dynamics at the unactuated end of the interconnection were dynamically augmented with a finite-dimensional exosystem modeling possible trajectory and disturbance inputs. The control design is based on the backstepping methodology, and stability analysis is done in the frequency domain. We use a similar approach to design an observer for state estimation and disturbance reconstruction. We guaranteed the robustness of the resulting output feedback controller using filtering techniques. This approach is illustrated in simulation on two test cases. These simulations raised some potential numerical limitations. Consequently, we should investigate model reduction techniques to ease the implementation of the proposed control strategies. Future contributions could also focus on leveraging the proposed assumptions.

Acknowledgements

The authors would like to thank the organizers of the 3rd DECOD Workshop, who allowed a preliminary version of this paper to be published as a chapter in [7] (p. 143-169).

References

[1] O.M Aamo. Disturbance rejection in 2x2 linear hyperbolic systems. *IEEE Transactions on Automatic Control*, 58(5):1095–1106, May 2013.

[2] U. J. F. Aarsnes, F. Di Meglio, and R. Shor. Avoiding stick slip vibrations in drilling through startup trajectory design. *Journal of Process Control*, 70:24–35, 2018.

[3] U. J. F. Aarsnes and N. van de Wouw. Axial and torsional self-excited vibrations of a distributed drill-string. *Journal of Sound and Vibration*, 444:127–151, 2019.

[4] J. Auriol. *Robust design of backstepping controllers for systems of linear hyperbolic PDEs*. PhD thesis, PSL Research University, 2018.

[5] J. Auriol and F. Bribiesca Argomedo. Observer design for n + m linear hyperbolic ODE-PDE-ODE systems. *IEEE control systems letters*, 7:283–288, 2023.

[6] J. Auriol, F. Bribiesca Argomedo, and F. Di Meglio. Robustification of stabilizing controllers for ODE-PDE-ODE systems: A filtering approach. *Automatica*, 147, 2023.

[7] J. Auriol, J. Deutscher, G. Mazanti, and G. Valmorbida, editors. *Advances in distributed parameter systems*, volume 14. Springer, 2022.

[8] J. Auriol and F. Di Meglio. An explicit mapping from linear first order hyperbolic PDEs to difference systems. *Systems & Control Letters*, 123:144–150, 2019.

[9] J. Auriol, N. Kazemi, K. Innanen, and R. Shor. Combining formation seismic velocities while drilling and a PDE-ODE observer to improve the drill-string dynamics estimation. In *2020 American Control Conference (ACC)*, pages 3120–3125. IEEE, 2020.

[10] G. Bastin and J-M. Coron. Further results on boundary feedback stabilisation of 2×2 hyperbolic systems over a bounded interval. In *8th IFAC Symposium on Nonlinear Control Systems, Bologna, Italy*, pages 1081–1085, September 2010.

[11] G. Bastin and J.-M. Coron. *Stability and boundary stabilization of 1-D hyperbolic systems*. Springer, 2016.

[12] D. Bou Saba, F. Bribiesca Argomedo, M. Di Loreto, and D. Eberard. Backstepping stabilization of 2×2 linear hyperbolic PDEs coupled with potentially unstable actuator and load dynamics. In *IEEE 56th Annual Conference on Decision and Control (CDC)*, pages 2498–2503, 2017.

[13] D. Bou Saba, F. Bribiesca-Argomedo, M. Di Loreto, and D. Eberard. Strictly proper control design for the stabilization of 2×2 linear hyperbolic ODE-PDE-ODE systems. In *2019 IEEE 58th Conference on Decision and Control (CDC)*, pages 4996–5001, 2019.

[14] J.-M. Coron, L. Hu, and G. Olive. Finite-time boundary stabilization of general linear hyperbolic balance laws via Fredholm backstepping transformation. *Automatica*, 84:95–100, 2017.

[15] J. Deutscher. Output regulation for general linear heterodirectional hyperbolic systems with spatially-varying coefficients. *Automatica*, 85:34–42, 2017.

[16] J. Deutscher and J. Gabriel. Robust state feedback regulator design for general linear heterodirectional hyperbolic systems. *IEEE transactions on automatic control*, 63(8):2620–2627, 2018.

[17] J. Deutscher and J. Gabriel. A backstepping approach to output regulation for coupled linear wave–ODE systems. *Automatica (2021)*, 123:109338, 2021.

[18] J. Deutscher, N. Gehring, and R. Kern. Output feedback control of general linear heterodirectional hyperbolic ode–pde–ode systems. *Automatica*, 95:472–480, 2018.

[19] J. Deutscher, N. Gehring, and R. Kern. Output feedback control of general linear heterodirectional hyperbolic ODE-PDE-ODE systems. *Automatica*, 95:472–480, 2018.

[20] F. Di Meglio, F. Bribiesca Argomedo, L. Hu, and M. Krstic. Stabilization of coupled linear heterodirectional hyperbolic PDE–ODE systems. *Automatica*, 87:281–289, 2018.

[21] F. Di Meglio, P.-O. Lamare, and U. J Aarsnes. Robust output feedback stabilization of an ODE–PDE–ODE interconnection. *Automatica*, 119:109059, 2020.

[22] B. A. Francis and W. M. Wonham. The internal model principle for linear multivariable regulators. *Applied mathematics and optimization*, 2(2):170–194, 1975.

[23] N. Gehring. A systematic design of backstepping-based state feedback controllers for ODE-PDE-ODE systems. *IFAC-PapersOnLine*, 54(9):410–415, 2021. 24th International Symposium on Mathematical Theory of Networks and Systems MTNS 2020.

[24] M. E. Guerrero, D. A. Mercado, R. Lozano, and C. D. García. Passivity based control for a quadrotor UAV transporting a cable-suspended payload with minimum swing. In *2015 54th IEEE Conference on Decision and Control (CDC)*, pages 6718–6723, 2015.

[25] J.K. Hale and S.M. Verduyn Lunel. *Introduction to functional differential equations*. Springer-Verlag, 1993.

[26] L. Hu, F. Di Meglio, R. Vazquez, and M. Krstic. Boundary exponential stabilization of 1-D inhomogeneous quasilinear hyperbolic systems. *arXiv preprint arXiv:1512.03539*, 2015.

[27] A. Irscheid, N. Espitia, W. Perruquetti, and W. Rudolph. Prescribed-time control for a class of semilinear hyperbolic PDE-ODE systems. *IFAC-PapersOnLine*, 55(26):47–52, 2022. 4th IFAC Workshop on Control of Systems Governed by Partial Differential Equations CPDE 2022.

[28] A. Irscheid, N. Gehring, J. Deutscher, and J. Rudolph. Tracking control for 2 x 2 linear heterodirectional hyperbolic PDEs that are bidirectionally coupled with nonlinear ODEs. In *Advances in distributed parameter systems*, volume 14, pages 119–144. Springer, 2022.

[29] R. Kern, N. Gehring, J. Deutscher, and M. Meissner. Design and experimental validation of an output feedback controller for a pneumatic system with distributed parameters. In *18th International Conference on Control, Automation and Systems (ICCAS)*, pages 1391–1396, 2018.

[30] M. Krstic and A. Smyshlyaev. Backstepping boundary control for first-order hyperbolic PDEs and application to systems with actuator and sensor delays. *Systems & Control Letters*, 57(9):750–758, 2008.

[31] M. Krstic and A. Smyshlyaev. *Boundary control of PDEs: A course on backstepping designs*, volume 16. Siam, 2008.

[32] H. Logemann, R. Rebarber, and G. Weiss. Conditions for robustness and nonrobustness of the stability of feedback systems with respect to small delays in the feedback loop. *SIAM Journal on Control and Optimization*, 34(2):572–600, 1996.

[33] P. Moylan. Stable inversion of linear systems. *IEEE Transactions on Automatic Control*, 22(1):74–78, 1977.

[34] J. Redaud, J. Auriol, and S.-I. Niculescu. Recursive dynamics interconnection framework applied to angular velocity control of drilling systems. In *2022 American Control Conference (ACC)*, pages 5308–5313, 2022.

[35] C. Schmuck, F. Woittennek, A. Gensior, and J. Rudolph. Flatness-based feed-forward control of an HVDC power transmission network. In *Telecommunications Energy Conference (INTELEC), 2011 IEEE 33rd International*, pages 1–6. IEEE, 2011.

[36] O. Smith. A controller to overcome dead time. *ISA J.*, 6:28–33, 1959.

[37] T. Strecker, O. M. Aamo, and M. Cantoni. Predictive feedback boundary control of semilinear and quasilinear 2 × 2 hyperbolic pde–ode systems. *Automatica*, 140:110272, 2022.

[38] N-T. Trinh, V. Andrieu, and C-Z. Xu. Output regulation for a cascaded network of 2 × 2 hyperbolic systems with PI controller. *Automatica*, 91:270–278, 2018.

[39] R. Vazquez, J.-M. Coron, M. Krstic, and G. Bastin. Local exponential H^2 stabilization of a 2×2 quasilinear hyperbolic system using backstepping. In *2011 50th IEEE Conference on Decision and Control and European Control Conference (CDC-ECC)*, pages 1329–1334. IEEE, 2011.

[40] R. Vazquez, M. Krstic, and J.-M. Coron. Backstepping boundary stabilization and state estimation of a 2×2 linear hyperbolic system. In *Decision and Control and European Control Conference (CDC-ECC), 2011 50th IEEE Conference on*, pages 4937–4942. IEEE, 2011.

[41] J. Wang and M. Krstic. Delay-compensated control of sandwiched ODE-PDE-ODE hyperbolic systems for oil drilling and disaster relief. *Automatica*, 120:109131, 2020.

[42] J. Wang and M. Krstic. Event-triggered output-feedback backstepping control of sandwich hyperbolic pde systems. *IEEE Transactions on Automatic Control*, 67(1):220–235, 2021.

[43] J. Wang and M. Krstic. Output-feedback control of an extended class of sandwiched hyperbolic PDE-ODE systems. *IEEE transactions on automatic control*, 66(6):2588–2603, 2021.

[44] J. Wang, M. Krstic, and Y. Pi. Control of a 2×2 coupled linear hyperbolic system sandwiched between 2 odes. *International Journal of Robust and Nonlinear Control*, 28(13):3987–4016, 2018.

[45] K. Yoshida. *Lectures on differential and integral equations*, volume 10. Interscience Publishers, 1960.